UNIVERSITY OF MESSINA

DEPARTMENT OF BIOMEDICAL SCIENCES AND MORPHOLOGICAL AND FUNCTIONAL IMAGES

PhD in TRANSLATIONAL MOLECULAR MEDICINE AND SURGERY

Cycle XXXV

Coordinator: Prof. Gaetano Caramori

S.S.D. BIO/14

ANTAGONIZING MIRNA TARGETING THE WNT PATHWAY TO TREAT PRIMARY AND SECONDARY OSTEOPOROSIS.

PhD Thesis

Luana Vittoria Bauso

Tutor:

Prof. Alessandra Bitto

ACADEMIC YEAR 2021-2022

INDEX

INTRODUCTION

Osteoporosis is a para-physiological condition in which the skeleton undergoes progressive loss of bone mass and qualitative alterations (macro and microarchitecture), leading to increased fragility and, as a result, a higher risk of spontaneous fractures (especially in vertebrae, femur, wrist, humerus, ankle) or due to minor trauma[1]. Bone loss is determined by an alteration of the dynamic balance of bone remodelling, in which bone resorption mediated by osteoclasts exceeds the osteoblastic activity of bone formation[2].

In this context, Runt-related transcription factor 2 (Runx2) is the earliest osteoblastic marker, required for osteoblastic differentiation. In turn, it promotes the expression of genes encoding osteocalcin, VEGF, RANKL, and sclerostin[3]. Another transcription factor required for osteoblast maturation is Osterix[4]. Various factors including bone morphogenetic proteins (BMPs), fibroblast growth factor (FGF), insulin-like growth factor (IGF), and parathyroid hormone (PTH), also influence osteoblast proliferation and differentiation[5]. Moreover, PTH and BMP activity is linked to the stimulation of Wnt signaling pathways involved in bone metabolism[6]. Mature osteoblasts express first alkaline phosphatase (ALP) and type I collagen, both required for bone matrix synthesis and mineralization, and then release other mineralization regulators such as osteocalcin, osteopontin, and ostenectin, as well as RANKL (Receptor Activator of Nuclear factor kappa-B ligand) and PTH receptor (PTHR1) that are essential for osteoclast differentiation[7]. Finally, osteoblasts differentiate into osteocytes embedded in the mineralized matrix[8].

Depending on the factors that influence bone metabolism, osteoporosis can be classified into primary or secondary. Osteoporosis is defined as primary when associated with the physiological loss of bone mass, and in turn can occur in the post-menopausal form, when

directly caused by an estrogenic deficiency, or in the senile one, if associated with aging processes. Instead, it is known as secondary osteoporosis when determined by other conditions such as endocrine, gastrointestinal, or blood diseases, drugs that interfere with bone metabolism, lifestyle, etc.[9].

The most frequent form of primary osteoporosis is certainly the postmenopausal one, in which the reduced action of estrogens negatively affects bone metabolism. In fact, by interacting with its own receptors, estrogens act at the cellular level promoting osteoblast proliferation and differentiation by activating Wnt signal[10], stimulating collagen production, and reducing the activity of osteoclasts by promoting apoptosis and by negatively regulating the expression of RANKL, and cytokines such as IL-1, IL-6 and TNF, which promote osteoclastogenesis. Furthermore, estrogens activate the calcitonin secretion while inhibiting that of PTH, thus reducing the process of bone resorption modulated by these two hormones, and also promote the conversion of vitamin D3 into its active form, which favors the intestinal and renal absorption of calcium, in addition to its deposition in the bone[11] (Figure 1).

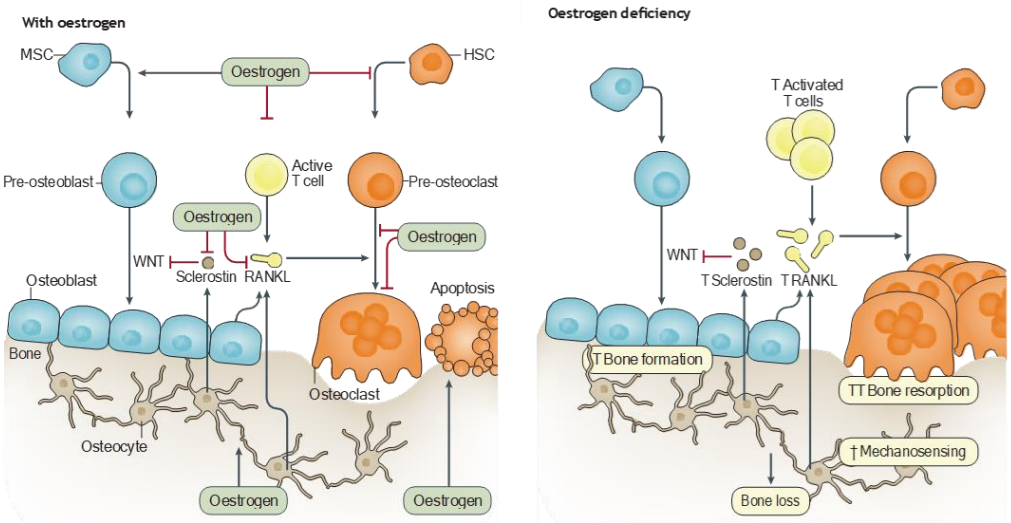

Figure 1. *Pathway diagram of the estrogen modulation of bone metabolism.*

On the other hand, among the secondary forms, the most common is the glucocorticoid-induced osteoporosis (GIO), due to the interference that these drugs (widely used for the treatment of several inflammatory diseases) have with bone metabolism[12]. In particular, glucocorticoids may have a direct effect on bone formation by upregulating the expression of peroxisome proliferator-activated receptor gamma 2 (PPARγ2) which promotes the differentiation of multipotent precursor cells into adipocytes rather than osteoblasts, thus reducing the number of osteoblasts[13]. Furthermore, by stimulating the overexpression of sclerostin which binds to the co-receptors for Lrp4 and Lrp5[14], glucocorticoids have a direct inhibitory effect on the Wnt/β-catenin signaling pathway resulting in reduced osteogenic differentiation and an increase in apoptosis[15]. On the other hand, the direct effects on osteoclasts are aimed at the RANKL/OPG (osteoprotegerin) system, with an increase in the expression of RANKL, essential for the differentiation, survival and function of osteoclasts, and a reduced expression of OPG, a natural antagonist of RANKL, resulting in an increase in osteoclast activity and, consequently, a prevalence of bone resorption processes[16]. Glucocorticoids can also have indirect effects on bone metabolism by reducing calcium absorption in both the intestine and the kidney, and by reducing the production of growth hormone (GH), IGF1 and IGF1 binding protein (IGF-BP), which are crucial for maintaining bone homeostasis[17] (Figure 2).

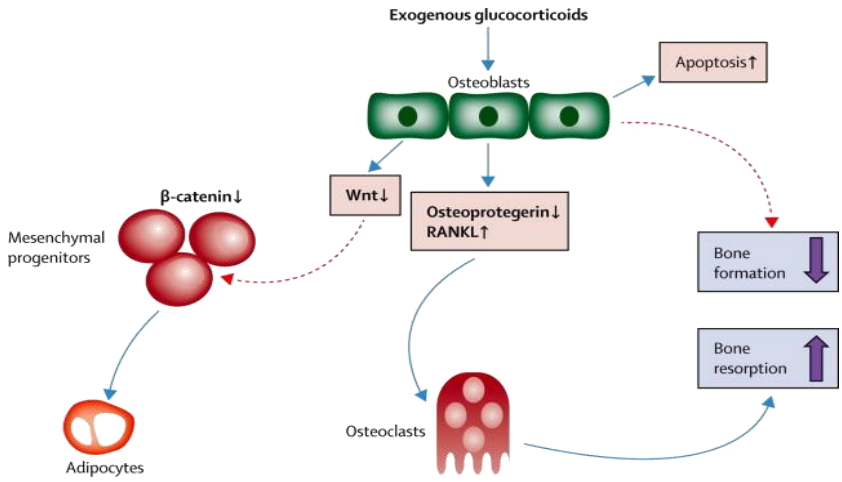

Figure 2. *Pathway diagram of the glucocorticoid modulation of bone metabolism.*

Osteoporosis is now known to represent a global public health problem, with over 200 million people affected worldwide and an incidence of 1 in 3 women and 1 in 5 men over the age of 50. It causes significant morbidity and, in some cases, even mortality. Furthermore, osteoporosis leads to a decrease in the quality of life, in addition to the high economic costs of the health system to ensure patient care[18].

Although osteoporosis has traditionally been considered a women's medical issue, it is a serious public health problem also in men, who develop osteoporosis as a result of a complex combination of factors such as age-related hypogonadism, hereditary factors, physical inactivity, smoking, alcohol abuse, and corticosteroid excess[19]. Osteoporosis in men is far underestimated, although not only morbidity and mortality rates associated with osteoporotic fractures are higher in men than in women[20], but also pharmacological treatments currently available are restricted to bisphosphonates, teriparatide (for up to two years), and testosterone therapy[21].

Therefore, a successful therapeutic approach to treating osteoporosis in both women and men must be identified immediately.

Currently, the pharmacological treatment of osteoporosis involves the use of two categories of drugs: antiresorptive drugs which reduce bone absorption by affecting osteoclastic activity, and anabolic drugs which stimulate bone formation and mineralization. These drugs are generally combined with calcium supplement and vitamin D, which enhances calcium intestinal reabsorption and directly stimulates osteoblastic activity[22].

Among the antiresorptive drugs, we can mention:

- bisphosphonates (alendronate, ibandronate, risedronate and zoledronic acid), which represent the first line drugs used for the treatment of osteoporosis even if they have several side effects such as hypocalcemia, fever, widespread pain, alterations in renal function, osteonecrosis of the jaw [23];
- denosumab, a monoclonal antibody that acts by blocking the binding of RANKL to its RANK receptor expressed by osteoclasts, inhibiting their differentiation, activation and survival, although it is not used as a first-line drug and may increase the risk of osteonecrosis of the jaw and skin infections [24];
- calcitonin, which, despite having minor side effects (nausea, abdominal pain, hypersensitivity reactions, skin rashes), appears to have limited efficacy[25];
- hormone replacement therapy (HRT) with estrogens to treat postmenopausal osteoporosis, although this type of therapy exposes patients to a greater risk of developing cardiovascular problems and breast cancer[26].
- Selective Estrogen Receptor Modulators (SERMs), such as raloxifene and bazedoxifene, which are selective agonists of estrogen receptors located in some tissues like bone, where they promote anti-resorptive activity, while they act as antagonists in other tissues such as breast and uterus, thus reducing the risk of

developing neoplasms. However, the use of these drugs can produce serious side effects like venous thromboembolism[27].

Currently, the only anabolic drugs that exclusively promotes new bone formation are:

- teriparatide, the 1-34 N-terminal portion of the PTH molecule produced by recombinant DNA technology, which stimulates osteogenesis through direct effects on osteoblasts. Unfortunately, teriparatide shows important limits in the duration of treatment (maximum 24 months) and in the economic cost which is higher than all the other drugs available. Therefore, the use of teriparatide is only recommended for secondary prevention in patients with severe osteoporosis[28];
- romosozumab, monoclonal antibody neutralizing sclerostin, physiological inhibitor of the Wnt system involved in osteogenesis, which seems to have a considerable and rapid beneficial effect on bone mass. However, this effect decreases after 12 monthly administrations, which is why it is only indicated for the treatment of women with severe postmenopausal osteoporosis and a high risk of fracture[29].

In addition to the two categories of drugs mentioned above, there are also the Dual Action Bone Agents (DABA), which have a dual action as they work both by decreasing resorption and increasing the production of new bone tissue[30]. This category is represented by strontium ranelate, a synthetic strontium salt which stimulates osteoblastic formation by interacting with the Calcium Sensing Receptor (CaSR) and, at the same time, reduces osteoclastic production by increasing the production of OPG[31]. Nevertheless, treatment with strontium ranelate is limited to osteoporotic patients with a high risk of fractures, as its use increases the risk of thromboembolic events[32].

Therefore, it is clear that the treatment of osteoporosis mainly prefers the use of anti-resorptive drugs, which only slow down the rate of bone loss without increasing bone mass, and could even cause serious side effects. On the other hand, among the few anabolic agents available, a drug that has a long-term effectiveness and does not cause undesirable events has not yet been identified.

Hence, signals and mechanisms that target bone-forming cells or their progenitors in order to restore bone strength and density are, today, of great therapeutic interest.

In this context, the Wnt signaling pathway has emerged as a crucial regulator of bone metabolism, recently drawing the interest of numerous researchers in investigating an anabolic therapeutic approach that targets this pathway[33].

Wnt signaling was first recognized to be implicated in carcinogenesis and in embryonic development[34]. Wnt proteins constitute a large family of secreted ligands that are involved in several cellular processes including proliferation, differentiation, survival, migration and polarity. To date, 19 members of the Wnt family and 10 related seven-pass transmembrane receptors belonging to the Frizzled family (Fz) have been identified in both humans and mice, in addition to Ror2, Ryk, and 2 low density lipoprotein receptor-related proteins (LRPs) such as LRP5 and LRP6[35].

Different Wnts bind to specific receptors and so selectively activate three distinct Wnt cascades: the Wnt/β-catenin pathway, also called canonical Wnt pathway, the non-canonical Wnt pathway, and the Wnt-calcium pathway. However, the Wnt/β-catenin pathway has emerged as the main Wnt cascade that affects bone cells[36] (Figure 3).

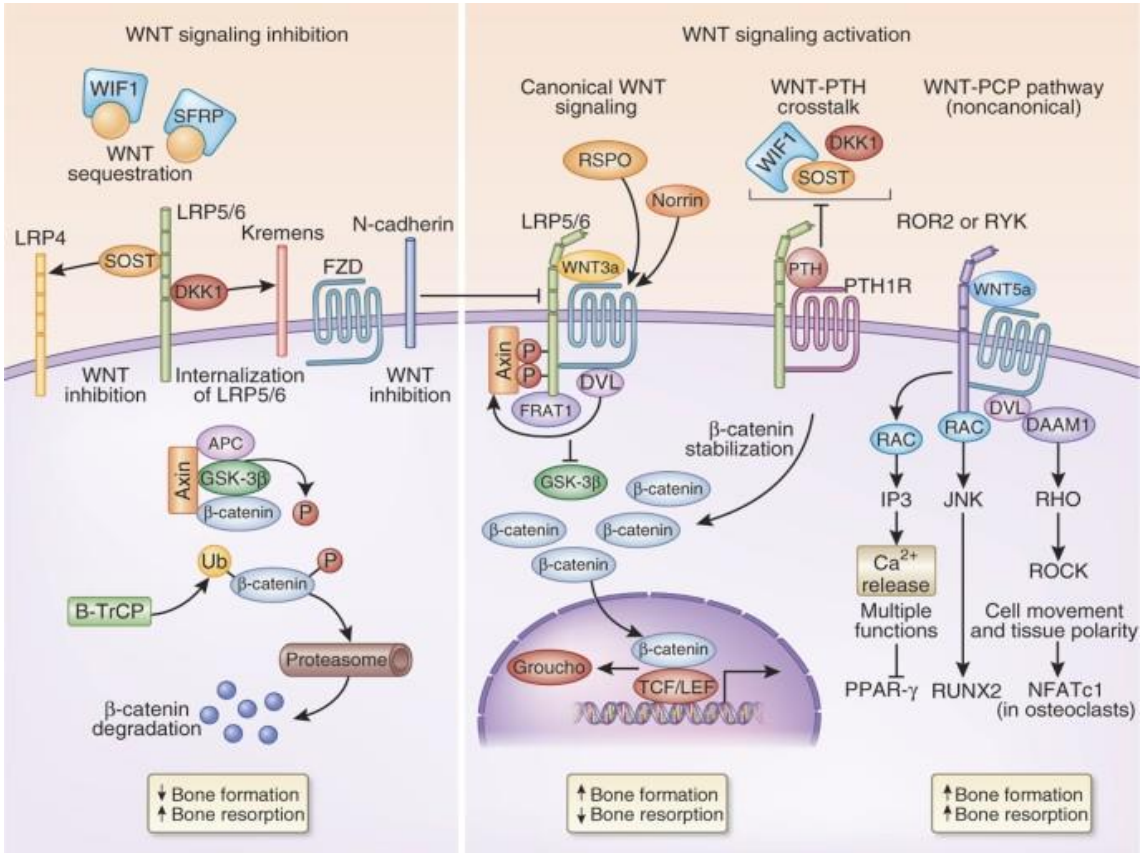

Figure 3. *Pathway diagram of the Wnt cascades and their involvement in bone metabolism.*

The canonical pathway begins with a Wnt protein binding to a receptor complex consisting of a Fz and either LRP5 or LRP6, leading to the recruitment of Axin to the Wnt/receptor complex and the consequent inactivation of the destruction complex initially formed by Axin, adenomatosis polyposis coli (APC), protein phosphatase 2A (PP2A), glycogen synthase kinase 3 (GSK3) and casein kinase 1α (CK1α). The inactivation of the destruction complex prevents the ubiquitin-mediated proteasomal degradation of β-catenin which, once accumulated in the cytoplasm, translocates into the nucleus and activates the lymphoid enhancer factor (Lef)/T-cell factor (Tcf) complex of transcription factors which induce a specific cellular response[37].

Several studies have shown that the canonical Wnt pathway affects both osteoblastic and osteoclastic lineage. In particular, it has been found to promote mesenchymal stem cells (MSC) differentiation along the osteoblastic line while suppressing differentiation along the chondrogenic and adipogenic lines[38], and to prevent the apoptosis of mature osteoblasts[39]. It also inhibits the differentiation of osteoclasts by promoting the production and secretion of OPG[40] and, even if the mechanism is still unclear, it has been observed that the deletion of β-catenin in osteoclasts results in an increase in their number[41].

Various Wnt proteins have been shown to play a crucial role in bone homeostasis. Among these, Wnt10b appears to be the most important endogenous regulator of bone mass by improving osteoblastogenesis[42], followed by Wnt6 and Wnt10a, which promote the differentiation of mesenchymal stem cells into osteoblasts rather than adipocytes via the canonical Wnt pathway[43]. Recent studies have also shown that Wnt1 mutations lead to a reduced induction of Wnt signaling, impairing the bone formation process[44]. Wnt16 has been found to stimulate the canonical Wnt signaling pathway in osteoblasts and suppress osteoclast maturation by upregulating OPG expression[45]. Furthermore, loss-of-function mutations in LRP5 and LRP6 have been related to a decrease in bone mass, confirming the importance of the canonical Wnt pathway in bone formation[46]. On the other hand, loss-of-function mutations in the gene encoding Sclerostin (SOST) prevent it from inhibiting the canonical Wnt pathway, resulting in increased bone density[47].

Recent studies have revealed the relevance of β-catenin in influencing bone formation via Wnt signaling by regulating both osteoblast and osteoclast lineages. The effective target genes of β-catenin during osteoblast differentiation remain largely unknown, although β-catenin has been found to directly induce Runx2[48] and OPG expression[49]. So, the importance of β-catenin in Wnt-mediated bone homeostasis is well-established. However, although Wnt3a preferentially activates canonical Wnt signaling in bone homeostasis[50],

it has been shown to enhance osteoblast differentiation by activating non-canonical Wnt signaling, as well as Wnt4[51], Wnt5a[52], and Wnt7b[53], thus elucidating the role of β-catenin independent Wnt signaling in bone formation.

Wnt signaling is constantly modulated at several points along its pathway to ensure an appropriate function. As a result, several Wnt inhibitors affect the signaling pathway, including: the secreted frizzled-related proteins (sFRPs), which occupy the Wnt-binding site of Frizzleds; the Wnt inhibitory factor 1 (Wif-1), which directly binds to Wnt proteins; Dickkopfs (Dkk), Wise and Sclerostin that interact with LRP5 or LRP6[54].

In this context, microRNAs (miRNAs) are also important in modulating the Wnt pathway and avoiding its hyperactivation. In turn, the Wnt pathway appears to be associated with miRNA synthesis and activity, interacting together to regulate many biological processes[55].

MicroRNAs (miRNAs) are small non-coding RNA molecules containing approximately 19-25 nucleotides that regulate gene expression at the post-transcriptional level[56], and are implicated in controlling various biological processes such as cell proliferation, apoptosis, metabolism, and differentiation, via base-pairing with complementary sequences within target mRNAs[57]. As a result, miRNAs have recently been identified as essential regulators of gene expression, and since a single miRNA potentially target several genes, miRNA dysregulation has been linked to a variety of diseases including cancer, autoimmune disorders, developmental disorders, and more[58].

MicroRNAs silencing may occur either by direct cleavage of their respective mRNA targets, degradation through deadenylation, or prevention of mRNA translation[59].

MiRNAs target mRNAs by complementary base-pairing binding multiple sites in 3′ untranslated regions (UTR). The "seed" sequence, a region of 6-8 nucleotides contained

in the 5' end of the miRNA from positions 2 to 8, facilitates binding of miRNA to target mRNA[60]. Additionally, the 3' UTR of a single target mRNA can exhibit several miRNA binding sites, as well as a single miRNA can control multiple target mRNAs by interacting with the corresponding binding site in their 3' UTRs[61].

RNA polymerase II/III (RNA Pol II/III) is responsible for miRNA transcription[62]. First, the Drosha - DGCR8 complex converts primary miRNA transcript (pri-miRNA)[63], which can be monocistronic or polycistronic, into the pre-miRNA, a hairpin-structured sequence of 60-70 nucleotides in length[64]. The pre-miRNA is then translocated from the nucleus to the cytoplasm, where Dicer cleaves it into a mature double-stranded miRNA[65]. Subsequently, the mature miRNA is incorporated into the RNA inducing silencing complex (RISC) which maintains the functional guide strand, while releasing the passenger strand which is finally destroyed[66]. When a mature single-strand miRNA associated with the RISC complex interacts with a target mRNA, it is directed to destroy it when the pairing is perfect, or prevent it from being translated when the match is incomplete, depending on the level of complementarity[67].

MiRNAs can also be secreted into extracellular fluids such as serum, cerebrospinal fluid, saliva, sperm, ovarian follicular fluid, breast milk, and carried to target cells by vesicles like exosomes or by binding-proteins like Argonautes. Extracellular miRNAs work as chemical messengers to facilitate cell-cell communication: miRNAs have hormone-like properties in this aspect[68].

In recent years, miRNAs have demonstrated enormous potential for diagnostic and therapeutic uses. In this regard, there are two alternatives to use miRNAs for therapeutic interventions, based on the use of exogenous miRNAs to replace endogenously generated miRNAs[69], or antagonists that reduce the gene regulatory function of biological

miRNAs[70]. In the first scenario, synthetic miRNA mimics are employed to imitate the beneficial regulatory function of some natural miRNAs. On the other hand, antagonistic oligonucleotides, also known as antagomirs, which target miRNAs that exhibit a negative effect on gene expression regulation, are a potential approach for the treatment of cancer and other disorders, including osteoporosis. They are single-stranded antisense oligonucleotides capable of trapping and destroying mature miRNAs due to its greater affinity or amount than the mRNA target[71].

Despite this, antisense oligonucleotides composed only of bases are rapidly destroyed in vivo by endo- and exonucleases[72], limiting interactions with their endogenous miRNA targets. The need to overcome these limits emerged immediately and for this reason several strategies based on chemical modifications of the antagomir were introduced[73]. The most typical and effective modified antagomirs are known as locked nucleic acids (LNAs), which include two methyl groups in the 2′-oxygen and 4′-carbon, giving a cyclic structure which improves their affinity for the target and keeps them from degradation, as well as reducing toxicity[74].

Recently, several studies have found that miRNAs can affect osteoblast differentiation by targeting the Wnt signaling pathway[75]. In particular, it has been shown that some miRNAs highly expressed during osteoporosis negatively affect the activation of the Wnt pathway. Similarly, miRNAs targeting Wnt inhibitors and which are found to be down-regulated in osteoporosis have been identified[76]. Among these, miR-9-5p was found to negatively regulate Wnt3a, inhibiting osteoblast differentiation and promoting osteoporosis progression[77,78].

MiR-376c, in addition to acting as a tumor suppressor that inhibits cell proliferation and invasion in osteosarcoma[79], also appears to be capable of suppressing osteogenesis.

Target prediction analysis tools and experimental validations identified Wnt3a as a direct target of miR-376c, preventing β-catenin transactivation and hence inhibiting bone formation[80].

MiR-374b-5p has been also identified as a key inhibitor of osteoblast development by targeting Wnt3a and RUNX2, considering that elevated levels in plasma have been linked to postmenopausal osteoporosis[81]. MiR-34a-5p, a Wnt signal inhibitor that target Wnt1[82], has been revealed to reduce osteoblastic maturation[83]. MiR-31-5p has been shown to reduce osteogenesis by affecting RUNX2 and Osterix expression[84], as well as to increase osteoclastogenesis by modulating RANKL[85]. It has also been found to interact with FZD3[86], inhibiting Wnt signaling, and predicted to bind to the 3'UTR of WNT1[87], suggesting that its involvement in bone homeostasis is mediated by Wnt signal. In addition, miR-31-5p was found to be up-regulated in an ovariectomized rat model[88] and in postmenopausal women[89].

MiR-199a-5p has been observed to inhibit cell proliferation and differentiation in some diseases by targeting FZD4 and Wnt2[90], and to positively regulate RANKL-induced osteoclast differentiation[91], although its involvement in osteoporosis is still controversial[92]. MiR-100, which has been found up-regulated in osteoporotic patients inhibiting osteoblast differentiation[93], could be associated to the Wnt pathway by potentially targeting FZD5 and FZD8[94].

MiR-16-3p is negative related to bone formation as it inhibits osteogenic differentiation by probably binding to the 3'UTR of WNT5A mRNA[95].

MiR-375 was found to reduce osteoblast differentiation by downregulating RUNX2 expression[96], and also Frizzled 8 has been identified as a target of miR-375[97]. As a result, miR-375 is probably involved in the control of osteogenesis via the Wnt pathway. MiR-

23a attenuates osteoblast maturation by suppressing expression of RUNX2[98], and is probably linked to the inhibition of the Wnt receptor LRP5[99].

MiR-409-5p was identified as an inhibitor of osteoblast function by targeting Lrp-8, an activator of the canonical Wnt cascade, by demonstrating that silencing miR-409-5p improves bone microarchitecture in ovariectomized mice[100].

MiR-214 was found to be significantly increased in osteoporosis patients[101], suggesting its relevance in bone metabolism. Furthermore, an in vitro investigation indicated that miR-214 reduces osteoblast differentiation and β-catenin expression, confirming bioinformatics analysis that revealed the complementary affinity with the 3'-UTR of β-catenin mRNA[102,103].

Overexpression of miR-139-5p, which exerts its role by targeting FZD4 and β-catenin[104], has been found to impair osteoblast differentiation. NOTCH1, which acts as an effector of the Wnt canonical pathway, is also another potential target of miR-139-5p[105].

Both miR-141-3p and miR-22 have been shown to act as negative regulators of osteoblast proliferation and differentiation, by probably targeting β-catenin mRNA[106,107].

Other data suggests that while miR-26b-3p represses ER-α expression, which in turn reduces bone formation by inactivating the Wnt/β-catenin signal[108], miR-26b-5p activates the Wnt/β-catenin pathway by targeting GSK3β and stimulates osteogenesis[109], as well as miR-346, which directly targets the 3′ UTR of GSK3β promoting bone formation[110].

MiR-142-3p targets APC, causing the accumulation and nuclear translocation of β-catenin, which stimulates Wnt signaling and induces osteoblastogenesis[111].

MiR-27a-3p has been demonstrated to promote osteoblastic differentiation by inhibiting sFRP1[112] and APC[113], promoting the nuclear translocation of β-catenin which stimulates the expression of osteogenesis-related genes.

MiR-218 promotes osteoblast differentiation by directly targeting the 3′-UTR of DKK2 and SFRP2 mRNAs[114–116], which are known Wnt inhibitors.

MiR-29a-3p seems to mitigate bone loss in an in vivo model of glucocorticoid-induced osteoporosis[117], and to promote osteoblast differentiation in vitro, probably by targeting two Wnt antagonists, DKK1 and SFRP2[118].

It was demonstrated that miRNA-291a-3p enhances osteogenic differentiation in an in vitro model of dexamethasone-induced osteoporosis by directly inhibiting DKK1 translation and then activating the Wnt/β-catenin signaling pathway[119].

MiR-433-3p was shown to be down-regulated in an ovariectomized rat model of postmenopausal osteoporosis, considering that its target is represented by the Wnt antagonist DDK1[120].

MiR-335-5p also stimulates osteoblast differentiation[121] and inhibits apoptosis[122] by targeting DKK1[123]. MiR-539, which prevents β-catenin degradation by targeting AXIN1 and promotes osteoblast activity and osteoclast apoptosis, has been demonstrated to be down-regulated in osteoporotic rats[124].

MiR-542-3p appears to have a protective role in bone homeostasis, preventing osteoporosis in an in vivo model of ovariectomized rats by targeting the Wnt inhibitor SFRP1[125]. The let-7 miRNAs, a highly conserved family of microRNAs, were shown to have significant association with both Wnt pathway[126] and regulation of bone homeostasis [127], even if the molecular mechanisms remain still unclear.

Among these, let-7c was found to be overexpressed in osteoporotic patients and to inhibit osteoblastic differentiation in vitro by targeting the stearoyl-CoA desaturase-1 (SCD-1) [128,129], probably leading to a decreased activation of Wnt signal. Let-7i-3p also acts as an inhibitor of the canonical Wnt pathway by targeting LEF1, hence affecting osteogenesis[130].

Finally, both let-7d-5p and let-7g-5p have been demonstrated to block the Wnt pathway by targeting Wnt1[131] and the Wnt effector HMGA2 (High Mobility Group AT-Hook 2)[132], respectively, even if their involvement in osteoporosis is still unclear.

In summary, miRNAs that control the Wnt pathway by targeting Wnt activators are up-regulated in osteoporosis, while those miRNAs that target Wnt antagonists are down-regulated. Hence, these miRNAs could have a great potential as anabolic therapeutic agents for the treatment of osteoporosis by using the corresponding antagonists or mimics, depending on their beneficial or deleterious effects on bone, respectively.

Nevertheless, most of these findings probably require further validation both in vitro and in vivo, as well as greater data consistency, to better understand the link between miRNAs and Wnt signal implicated in bone metabolism.

For this reason, the aim of this PhD research project was to identify those microRNAs involved in primary and secondary osteoporosis that interfering with the Wnt/β-catenin signaling pathway could represent therapeutic targets for the treatment of osteoporosis.

The animal models selected in this study reproduce the most common forms of primary and secondary osteoporosis: postmenopausal osteoporosis and glucocorticoid-induced osteoporosis, respectively.

As first, ovariectomized animal model has been chosen since it is the most commonly used to simulate postmenopausal osteoporosis in vivo. In fact, several studies have revealed significant bone loss consequent to estrogen deficiency caused by ovariectomy, especially in the proximal tibial metaphysis, femoral neck, and lumbar vertebral body after 14, 30, and 60 days, respectively[133]. An alternative method to surgical ovariectomy leading to osteoporosis is the induction with pharmaceutical agents such as gonadotropin-releasing hormone agonists, estrogen receptor antagonists and aromatase inhibitors, which is reversible after withdrawal and thus requires continuous administrations to maintain the animal model. Other hormonal interventions that cause bone loss include hypophysectomy and parathyroidectomy, which are not only as invasive as ovariectomy, but they also do not directly affect estrogen levels and can cause other complications in the animals[134]. As a result, the ovariectomy model is the one that differs least from the real postmenopausal condition in women, as well as being the most reliable and ethically appropriate.

On the other hand, induction of osteoporosis through subcutaneous administration of high doses of prednisolone to C57BL/6J mice is the most represented GIO model, probably due to its lower potency than other glucocorticoids such as dexamethasone and methylprednisolone, which allows to reproduce the GIO model without causing serious bone injuries in the animal, or even death before the end of the induction. Furthermore, daily injections are stressful for the animals, and could interfere with the study. Therefore, the majority of studies carried out in GIO mice have predominantly employed slow-release subcutaneous pellets[135]. As a result, based on the scientific literature, a prednisolone dose of 5 mg/kg/day in a 60-day slow-release pellet was selected as GIO model of this study[136].

Finally, the antagomirs used in this study contain not only LNA nucleotides that enhance target affinity, but also a full phosphorothioate (PS) backbone that increases stability[137], biodistribution[138], and cellular uptake in vivo[139]. Furthermore, they are shorter (12-16 nt) than other antisense oligonucleotides (approximately 20 nt long), and hence enter considerably better through the natural mechanisms of cellular uptake[140]. In this way, this study was able to identify not only potential therapeutic targets, but also the efficacy of the selected antagomirs in the treatment of osteoporosis.

MATERIALS AND METHODS

Animal models

Fifty-one adult C57BL/6J mice (25-30 g), including 17 males, 24 females and 10 ovariectomized females, were purchased from Charles River Laboratories Italia s.r.l. (Calco, Italy) and maintained in plastic cages in the Animal Facility of the Department of Clinical and Experimental Medicine under controlled environmental conditions (12 h light-dark cycle, 22-24 °C), receiving free access to standard food and water. All procedures were carried out in accordance with the Directive 2010/63/EU and the ARRIVE guidelines for animal care and use, reviewed by the Ethics Committee of Messina University (OPBA), and approved by the Italian Ministry of Health.

In this study, two experimental models of osteoporosis were adopted: ovariectomized (OVX) mice were used to simulate post-menopausal osteoporosis, while mice treated with high doses of prednisolone were used to reproduce glucocorticoid-induced osteoporosis.

For the postmenopausal osteoporosis model, 12-week-old female mice were used by selecting a of OVX mice (n=10) and a group of non-ovariectomized mice, representing the Sham-OVX group (n=7). Animals were euthanized one month following ovariectomy.

For the GIO experimental model, 12-week-old mice were divided into 2 groups as follows: (1) GIO group (n= 10 males + 10 females), which was administered a daily dose of 5mg/kg of prednisolone (Sigma-Aldrich, Germany) for 60 days by subcutaneously implanting, every 14 days, micro-osmotic pumps (Model 1002, Alzet) which contained the drug (dissolved in a total volume of 100 µl), and released it into the body with a

pumping rate of 0.25 µL/hour; (2) Sham GIO group (n= 7 males + 7 females) was used as negative control.

All the animals group mentioned above were killed by cervical dislocation, then femurs were kept to establish osteoporosis by histological analysis while the rest of anterior and posterior limb bones were used to isolate osteoblasts for molecular investigations.

Osteoblast isolation from mice

To identify the specific miRNAs implicated in osteoporosis that affect the Wnt pathway, primary osteoblasts were isolated from long bones of C57BL6/J mice. Bones were kept in PBS until use, epiphyses removed and bone marrow flushed with PBS.

To remove all soft tissue, diaphysis were cut into 1-2 mm pieces, washed several times with PBS and incubated by gently shaking for 2 hours at 37°C in a 2 mg/ml collagenase II solution (Sigma-Aldrich, Germany) dissolved in Dulbecco's Modified Eagle Medium (DMEM) with 1% of Penicillin and Streptomycin (P/S). Then, bone pieces were rinsed three times with PBS and placed in six-well plates containing DMEM supplemented with 10% Fetal Bovine Serum (FBS), 1% P/S, and 1% Amphotericin B (Ampho B).

Cells were maintained under standard conditions (37°C and 5% CO2 atmosphere) and fresh medium was added every 2-3 days. Ten days after isolation, cells reached the optimal confluence to be collected for mRNA isolation, while the culture media were used to obtain miRNAs.

Isolation of RNA from osteoporosis-induced mice osteoblasts, cDNA synthesis and Real-Time quantitative PCR (RT-qPCR) Amplification using TaqMan Array

Upon reaching confluence, RNA was isolated from primary osteoblast cells by using Trizol LS reagent (Invitrogen, US) and quantified with a spectrophotometer (NanoDrop

Lite, Thermo Fisher Scientific, US). cDNA was synthetized from 2 µg of RNA for a final volume of 60 µL by using SuperScript IV VILO Master Mix (Invitrogen, US).

RT-qPCR was performed by combining cDNA sample with the TaqMan Fast Advanced Master Mix in a configurable TaqMan Array 96-well plate supplied by Thermo Fisher (US), according to the manufacturer's instructions, and by using a QuantStudio 7 Flex Real-Time PCR System (Applied Biosystems, US) to measure amplification. Twenty nanograms of cDNA were loaded to each well of the plate, which was intended to contain 96 Taqman probes that specifically target transcript related to osteoporosis or the Wnt pathway. All the targets selected to configure the plate are listed in the table below (Table 1). B2m, 18s rRNA, Gapdh, Gusb, Actb, and Hprt were used as endogenous controls.

Gene Symbol	Gene Name	Assay ID
Dkk3	dickkopf homolog 3 (Xenopus laevis)	Mm00443800_m1
Wnt2	wingless-type MMTV integration site family, member 2	Mm00470018_m1
Dvl2	dishevelled 2, dsh homolog (Drosophila)	Mm00432899_m1
Sfrp4	secreted frizzled-related protein 4	Mm00840104_m1
Gsk3b	glycogen synthase kinase 3 beta	Mm00444911_m1
Frat1	frequently rearranged in advanced T cell lymphomas	Mm00484502_s1
Dvl1	dishevelled, dsh homolog 1 (Drosophila)	Mm00438592_m1
Axin1	axin 1	Mm01299060_m1
Fzd3	frizzled homolog 3 (Drosophila)	Mm00445423_m1
Fzd2	frizzled homolog 2 (Drosophila)	Mm02524776_s1
Sfrp1	secreted frizzled-related protein 1	Mm00489161_m1
Lrp6	low density lipoprotein receptor-related protein 6	Mm00999795_m1
Dkk1	dickkopf homolog 1 (Xenopus laevis)	Mm00438422_m1
Wnt1	wingless-type MMTV integration site family, member 1	Mm01300555_g1
Ctnnb1	catenin (cadherin associated protein), beta 1	Mm00483039_m1
Wnt5b	wingless-type MMTV integration site family, member 5B	Mm01183986_m1
Fzd1	frizzled homolog 1 (Drosophila)	Mm00445405_s1

Fzd5	frizzled homolog 5 (Drosophila)	Mm00445623_s1
Wnt8a	wingless-type MMTV integration site family, member 8A	Mm01157914_g1
Wnt3a	wingless-type MMTV integration site family, member 3A	Mm00437337_m1
Wnt8b	wingless-type MMTV integration site family, member 8B	Mm00442108_g1
Lrp5	low density lipoprotein receptor-related protein 5	Mm01227476_m1
Fzd8	frizzled homolog 8 (Drosophila)	Mm01234717_s1
Wnt7b	wingless-type MMTV integration site family, member 7B	Mm01301717_m1
Wnt9a	wingless-type MMTV integration site family, member 9A	Mm00460518_m1
Wnt3	wingless-type MMTV integration site family, member 3	Mm00437336_m1
Wnt11	wingless-type MMTV integration site family, member 11	Mm00437327_g1
Wnt10a	wingless-type MMTV integration site family, member 10A	Mm00437325_m1
Fzd6	frizzled homolog 6 (Drosophila)	Mm00433387_m1
Apc	adenomatosis polyposis coli	Mm00545872_m1
Sfrp2	secreted frizzled-related protein 2	Mm01213947_m1
Wnt16	wingless-type MMTV integration site family, member 16	Mm00446420_m1
Wnt7a	wingless-type MMTV integration site family, member 7A	Mm00437356_m1
Fzd9	frizzled homolog 9 (Drosophila)	Mm01206511_s1
Wisp1	WNT1 inducible signaling pathway protein 1	Mm01200484_m1
Fzd4	frizzled homolog 4 (Drosophila)	Mm00433382_m1
Wnt5a	wingless-type MMTV integration site family, member 5A	Mm00437347_m1
Wnt2b	wingless-type MMTV integration site family, member 2B	Mm00437330_m1
Wif1	Wnt inhibitory factor 1	Mm00442355_m1
Wnt6	wingless-type MMTV integration site family, member 6	Mm00437353_m1
Axin2	axin2	Mm00443610_m1
Frzb	frizzled-related protein	Mm00441378_m1

Wnt4	wingless-type MMTV integration site family, member 4	Mm01194003_m1
Fzd7	frizzled homolog 7 (Drosophila)	Mm00433409_s1
Ccnd1	cyclin D1	Mm00432359_m1
Csnk1a1	casein kinase 1, alpha 1	Mm00521599_m1
Ctnnbip1	catenin beta interacting protein 1	Mm00517812_m1
Csnk2a1	casein kinase 2, alpha 1 polypeptide	Mm00786779_s1
Mmp7	matrix metallopeptidase 7	Mm00487724_m1
Lef1	lymphoid enhancer binding factor 1	Mm00550265_m1
Ppard	peroxisome proliferator activator receptor delta	Mm00803184_m1
B2m	beta-2 microglobulin	Mm00437762_m1
18s rRNA	18S ribosomal RNA	Hs99999901_s1
Gapdh	glyceraldehyde-3-phosphate dehydrogenase	Mm99999915_g1
Gusb	glucuronidase, beta	Mm00446953_m1
Actb	actin, beta	Mm00607939_s1
Hprt	hypoxanthine guanine phosphoribosyl transferase	Mm00446968_m1
Bmp7	bone morphogenetic protein 7	Mm00432102_m1
Pth1r	parathyroid hormone 1 receptor	Mm00441046_m1
Ctsk	cathepsin K	Mm00484039_m1
Il6ra	interleukin 6 receptor, alpha	Mm00439653_m1
Esr1	estrogen receptor 1 (alpha)	Mm00433149_m1
Esr2	estrogen receptor 2 (beta)	Mm00599821_m1
Col1a2	collagen, type I, alpha 2	Mm00483888_m1
Calcr	calcitonin receptor	Mm00432282_m1
Alpl	alkaline phosphatase, liver/bone/kidney	Mm00475834_m1
Spp1	secreted phosphoprotein 1 (osteopontin gene)	Mm00436767_m1
Bglap3	bone gamma-carboxyglutamate protein 3 (osteocalcin gene)	Mm00649782_gH
Bmp2	bone morphogenetic protein 2	Mm01340178_m1
Sost	sclerostin	Mm04208528_m1
Pth	parathyroid hormone	Mm00451600_g1
Wnt10b	wingless-type MMTV integration site family, member 10B	Mm00442104_m1
Col1a1	collagen, type I, alpha 1	Mm00801666_g1
Runx2	runt related transcription factor 2	Mm00501584_m1
Lrp1	low density lipoprotein receptor-related protein 1	Mm00464608_m1
Lep	leptin	Mm00434759_m1

Timp2	tissue inhibitor of metalloproteinase 2	Mm00441825_m1
Crtap	cartilage associated protein	Mm00517335_m1
Vdr	vitamin D receptor	Mm00437297_m1
Clcn7	chloride channel 7	Mm00442400_m1
Mmp2	matrix metallopeptidase 2	Mm00439498_m1
Casr	calcium-sensing receptor	Mm00443375_m1
Itga1	integrin alpha 1	Mm01306375_m1
Il6	interleukin 6	Mm00446190_m1
Itgb3	integrin beta 3	Mm00443980_m1
Tgfb1	transforming growth factor, beta 1	Mm01178820_m1
Ar	androgen receptor	Mm00442688_m1
Igfbp2	insulin-like growth factor binding protein 2	Mm00492632_m1
Igf1	insulin-like growth factor 1	Mm00439560_m1
Esrra	estrogen related receptor, alpha	Mm00433143_m1
Notch1	notch 1	Mm00435249_m1
Calca	calcitonin/calcitonin-related polypeptide, alpha	Mm00801463_g1
Bmp6	bone morphogenetic protein 6	Mm01332882_m1
Dkk2	dickkopf homolog 2 (Xenopus laevis)	Mm01322146_m1
Ppargc1a	peroxisome proliferative activated receptor, gamma, coactivator 1 alpha (PGC1a gene)	Mm01208835_m1
Scd1	stearoyl-Coenzyme A desaturase 1	Mm00772290_m1

Table 1. *List of the 96 TaqMan probes contained in the configurable TaqMan Array plate used to perform qPCR from osteoblast cell mRNA.*

Isolation of microRNAs from osteoblast culture media, cDNA synthesis and Real-Time quantitative PCR (RT-qPCR) Amplification using TaqMan Array

The microRNAs were isolated from the collected osteoblast culture media by using mirVana PARIS RNA and Native Protein Purification Kit (Invitrogen, US).

According to the manufacturer's protocol, 12 ng of each miRNA sample were collected to synthetize cDNA by using TaqMan MicroRNA Reverse Transcription Kit, pre-amplified and finally loaded on Custom TaqMan Array MicroRNA Cards supplied by

Thermo Fisher. Then, cards were put in a QuantStudio 7 Flex Real-Time PCR System (Applied Biosystems, US) to perfom qPCR.

TaqMan Array MicroRNA Cards were designed by inserting 32 probes selected from scientific literature which target miRNAs implicated in osteoporosis and Wnt signal. The list of the 32 miRNAs probes (Table 2) and their layout in the card (Figure 4) are shown below. The small nuclear RNA U6 (U6 snRNA) was used as endogenous control.

miRNA name	assay ID	Card position
mmu-let-7c	000379	1
mmu-miR-9	000583	2
mmu-miR-26b	000407	3
U6 snRNA	001973	CTL
mmu-miR-34a	000426	4
mmu-miR-142-3p	000464	5
mmu-miR-199a-5p	000498	6
mmu-miR-218	000521	7
mmu-miR-291a-3p	002592	8
mmu-miR-335-5p	000546	9
mmu-miR-346	001064	10
mmu-miR-375	000564	11
mmu-miR-409-5p	002331	12
mmu-miR-539	001286	13
mmu-miR-542-3p	001284	14
mmu-miR-23a	000399	15
mmu-miR-31	000185	16
mmu-miR-22	000398	17
mmu-miR-374b	001319	18
mmu-miR-16*	002489	19
mmu-miR-26b*	002444	20
mmu-miR-433*	001078	21
mmu-miR-27a*	002445	22
mmu-miR-29a*	002447	23
mmu-miR-376c*	002523	24
mmu-let-7i*	002172	25
mmu-miR-214*	002293	26
mmu-let-7d	002283	27
mmu-let-7g	002282	28
mmu-miR-100	000437	29
mmu-miR-139-5p	002289	30

mmu-miR-141*	002513	31

Table 2. *List of the 32 TaqMan probes contained in the Custom TaqMan Array MicroRNA Cards used to perform qPCR from miRNA released from osteoblast in culture media. Where the miRNA family is not reported, the presence or absence of "*" indicates -3p and -5p, respectively.*

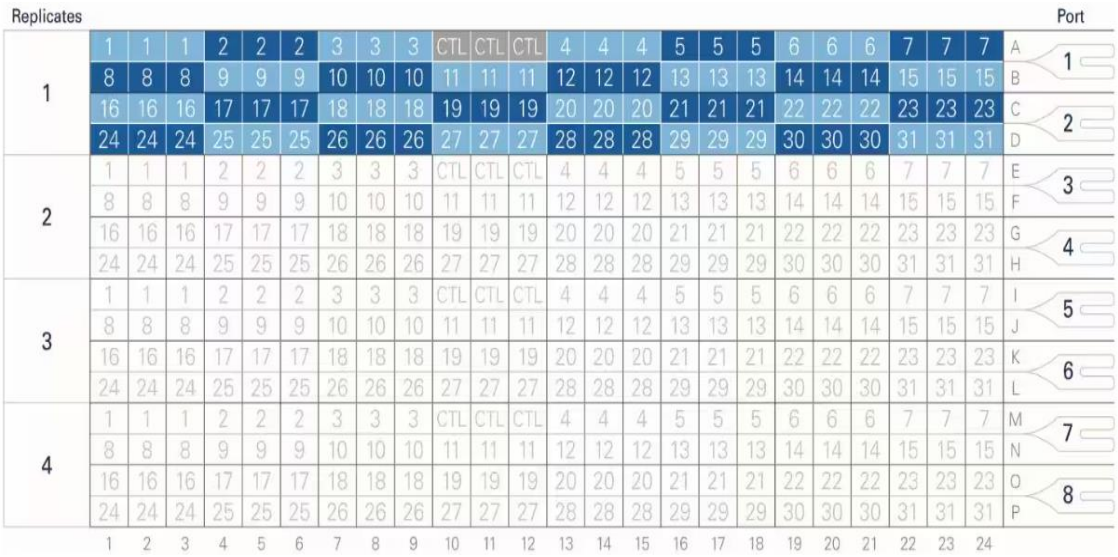

Figure 4. *Layout of the Custom TaqMan Array MicroRNA Cards. Replicates (1-4) refer to samples; for each replicate; probes from positions 1 to 31, including the control (CTL), are arranged in triplicate; each miRNA sample is loaded into the card through 2 ports.*

Bioinformatic Analysis

For bioinformatics analysis, each osteoporotic group was compared to its respective control group: OVX vs Sham females; GIO males vs Sham males; GIO females vs Sham females.

After eliminating samples that appeared to be outliers, ΔCq and ΔΔCq values were obtained for each comparison. ΔΔCq (ΔCq_{sample} - $\Delta Cq_{controls}$ mean) and ΔΔCq mean

(ΔCq_{sample} mean - ΔCqcontrols mean) were calculated for each sample and for each group, respectively.

The dysregulation of a gene that was consistently supported by the $\Delta\Delta$Cq of each single sample of the group was defined as 'highly supported', whereas the dysregulation of a gene that was only supported by the $\Delta\Delta$Cq mean of the group due to the intrinsic standard deviation was considered “poorly supported”.

The following data were obtained for each comparison:

- using the $2^{-\Delta\Delta Cq}$ method, the n-fold changes for each gene and miRNA differently expressed compared to the mean of the controls.
- using Pearson Correlation (P.C.), those genes with which miRNAs correlate positively (P.C. > 0.8). or negatively (P.C. < -0.8).

Seaborn, a data visualization library by Python based on matplotlib, was used to plot cluster maps, which are hierarchically-grouped heatmaps of the dataset based on a similarity algorithm.

Correlation matrices containing Pearson correlation coefficients between variables were also plotted using seaborn. Each cell of the matrix represents the correlation between two variables. Correlation coefficients range from -1 to 1, with values ranging from -0.8 to -1 indicating strong negative correlation, and values between 0.8 and 1 indicating strong positive correlation.

Antagomirs Design

Based on the bioinformatic analysis of the data obtained by qPCR, the following miRNAs that negatively affected the Wnt pathway were identified for each condition (ovariectomy

or GIO), then their sequences were obtained by using miRbase.org: mmu-miR-31-5p (5'-AGGCAAGAUGCUGGCAUAGCUG-3') and mmu-miR-199a-5p (5'-CCCAGUGUUCAGACUACCUGUUC-3') in the OVX group; mmu-miR-9-5p (5'-UCUUUGGUUAUCUAGCUGUAUGA-3') and mmu-miR-141-3p (5'-UAACACUGUCUGGUAAAGAUGG-3') in male GIO; mmu-let-7c-5p (5'-UGAGGUAGUAGGUUGUAUGGUU-3') in female GIO.

As a result, antagomirs have been designed in order to be reverse complementary to their respective miRNAs, and then produced through LNA technology (miRCURY LNA miRNA Inhibitors) by Exiqon (Denmark): I-MMU-MIR-31-5P CUSTOM MIRCURY (5'-TGCCAGCATCTTGCC-3'); I-MMU-MIR-199A-5P CUSTOM MIRCURY (5'-TAGTCTGAACACTGG-3'); I-MMU-MIR-9-5P CUSTOM MIRCURY (5'-GCTAGATAACCAAAG-3'); I-MMU-MIR-141-3P CUSTOM MIRCURY (5'-TCTTTACCAGACAGTG-3'); I-MMU-LET-7C-5P CUSTOM MIRCURY (5'-CATACAACCTACTACC-3'). Scramble antagomir (5'-ACGTCTATACGCCCA-3') has been also designed as negative control.

Animals treatment with antagomirs

Adult C57BL/6J mice (n=84) were purchased and cared as previously described, and then randomly assigned to groups to receive antagomirs.

For the postmenopausal osteoporosis model, 12-week-old female mice were divided into the following groups: OVX mice given I-MMU-MIR-31-5P (n=10); OVX mice administered with I-MMU-MIR-199A-5P (n=10); OVX mice receiving scramble (n=3); OVX mice taking only PBS as vehicle (n=7); Sham group (n=4) of non-ovariectomized mice, used as negative control.

Treatment began one month after ovariectomy, when osteoporosis emerged. Antagomirs, scramble and vehicle were administered intraperitoneally twice a week for 12 weeks. As suggested by the manufacturer's protocol, both lyophilized antagomirs and scramble were dissolved in PBS and injected in a final volume of 100 µL at a dose of 10 mg/kg during the first week, and 15 mg/kg for the remaining 11 weeks.

For the GIO model, 12-week-old mice were divided into the following groups: male GIO mice receiving I-MMU-MIR-9-5P (n=8); male GIO mice given I-MMU-MIR-141-3P (n=8); female GIO mice administered with I-MMU-LET-7C-5P (n=8); GIO mice taking scramble (n= 3 male + 3 female); GIO mice injected with PBS as vehicle (n= 6 male + 6 female); Sham group (n= 4 male + 4 female), which did not receive prednisolone treatment, as negative control.

GIO model was induced by administering prednisolone 5 mg/kg for 60 days using micro-osmotic pumps as previously described. Treatment started 30 days after GIO induction and consisted of twice-weekly intraperitoneal injections of antagomirs, scramble, or vehicle until the 60th day of GIO. As aforementioned, antagomirs and scramble were dissolved in PBS and administered in a final volume of 100 µL at 10 mg/kg for the first week, and 15 mg/kg from the second week until the end of prednisolone induction.

All the animals mentioned above were sacrificed by cervical dislocation. For further analysis, femurs were collected for histological evaluations and micro-CT scanning, to establish if the treatment with the selected antagomirs was able to reverse osteoporosis, and the rest of limb bones were used to isolate osteoblasts as mentioned above to evaluate through molecular investigations if the antagomir treatment changed the expression of genes involved in bone formation process.

RNA Isolation, cDNA synthesis and Real-Time quantitative PCR (RT-qPCR) Amplification from antagomir-treated mice osteoblasts

Upon reaching confluence, total RNA was isolated from treated mice osteoblasts as previously described. cDNA was synthetized from 1 μg of total RNA for a final volume of 20 μL using SuperScript IV VILO Master Mix (Invitrogen, US).

RT-qPCR was performed adding 1 μL of cDNA to the BlasTaq 2X qPCR MasterMix (Applied Biological Materials, Canada) in a final volume of 20 μL per well and using a QuantStudio 6 Flex Real-Time PCR System (Applied Biosystems, US) to measure amplification. Samples were loaded in triplicate and GAPDH was used as an endogenous control. The final concentration of the primers selected for the analysis was 10 μM.

Results were obtained using the $2^{-\Delta\Delta Cq}$ method and expressed as n-fold change in gene expression compared to the control group used as a calibrator. Runx2, Bmp6, and Col1a1 were used as target genes. Primers used for target and reference genes are reported below:

GAPDH forward, 5'-GTCAAGGCTGAGAATGGGAA-3'; GAPDH reverse, 5'-ATACTCAGCACCAGCATCAC-3'; Runx2 forward, 5'-GCCGGGAATGATGAGAACTA-3'; Runx2 reverse, 5'-GAACCGTCCACTGTCACTTT-3'; Bmp6 forward, 5'-CTCTTCGGGCTTCCTCTATC-3'; Bmp6 reverse, 5'-CCAACACCGACAGGATCT-3'; Col1a1 forward, 5'-AATGGTGCTCCTGGTATTGC-3'; Col1a1 reverse, 5'-GGCTCCTCGTTTTCCTTCTT-3'.

***Ex Vivo* Microcomputed Tomography**

To evaluate the effects of treatments on bone microstructure, the excised femurs were kept at -20°C until the micro-CT by usig in a micro-CT device (Skyscan 1174, Bruker,

Belgium). For micro-CT imaging, each femur was defrosted at room temperature and then scanned parallel to the sagittal and coronal plane.

The scanning parameters were set as follows: tube voltage (50 kV); tube current (200 µA); filter (Al 0.5 mm); image pixel size (7.3 µm); tomographic rotation (180°) with random movement; rotation step (0.5°).

Tomographic image reconstruction was performed using Skyscan Nrecon software (Bruker) with the following parameters: smoothing (2); smoothing kernel (Gaussian); ring artifact correction (5); beam hardening correction (33%); grey thresholds (62–70).

Micro-CT images were resliced parallel to the axial plane of the femoral distal epiphysis, CTAn Skyscan 1275 software (Bruker) was used to separate cortical and trabecular volumes, and perform 3D morphometric analysis on approximately 50 consecutive slices to determine bone volume fraction (bone volume/total volume, BV/TV, unit = %), and trabecular thickness (Tb.Th, unit = µm) by means of Batman tool.

Histological examination

Femurs were collected by disarticulating the leg at the hip and knee, and immediately fixed in 10% neutral buffered formalin at room temperature for at least 24 hours. After fixation, samples were cleaned of soft tissue and placed in a decalcifying solution (5 ml of 7% citric acid and 95 ml of 7.4% ammonium citrate, both dissolved in ddH2O, and a few drops of chloroform, for a total volume of 100 ml) for about 24 hours, dehydrated in graded ethanol, cleared in xylene, and then embedded in paraffin. Five-micron-thick paraffin-embedded horizontal bone sections were cut from the proximal end of the diaphysis, mounted on glass slides, deparaffinized, rehydrated, and stained with hematoxylin and eosin according to standard procedures for light microscopy. Femoral heads were observed to judge structural bone quality.

Statistical Analysis

All quantitative data are expressed as means ± S.D. Different groups were compared and analyzed using one-way ANOVA for non-parametric variables, with Tukey post-test for intergroup comparisons. Statistical significance was set at p values less than 0.05. Graphs were drawn using GraphPad Prism software version 9.0 for Windows (GraphPad Software Inc., US).

RESULTS

Identification of up- and down-regulated microRNAs and related mRNAs.

The bioinformatic analysis revealed which miRNAs were up- and down-regulated in each of the osteoporosis mouse models when compared to their respective Sham groups.

In particular, both miR-31 and miR-199a were found to be significantly up-regulated in the ovariectomized mice group when compared to the Sham group (Figure 5). In contrast, the following miRNAs were found to be down-regulated in ovariectomized mice: miR-100, miR-214*, miR-23a, miR-26b*, miR-27a*, miR-335, miR-539, miR-542-3p, miR-16*, and miR-291a-3p (Figure 6).

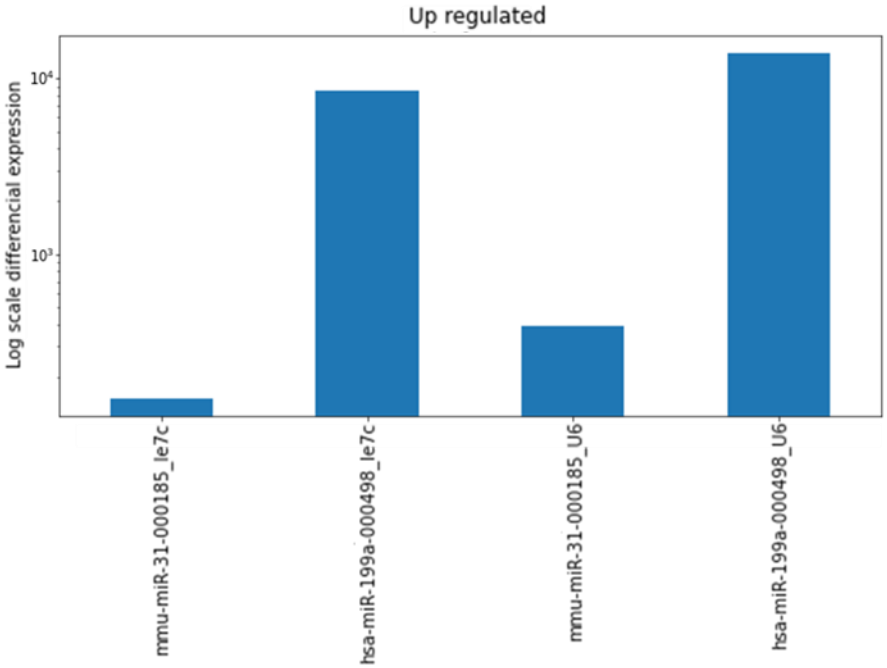

Figure 5. *Expression of up-regulated microRNAs in ovariectomized mice compared to Sham group. The expression levels are represented on a logarithmic scale and normalized using let7 and U6 as endogenous controls.*

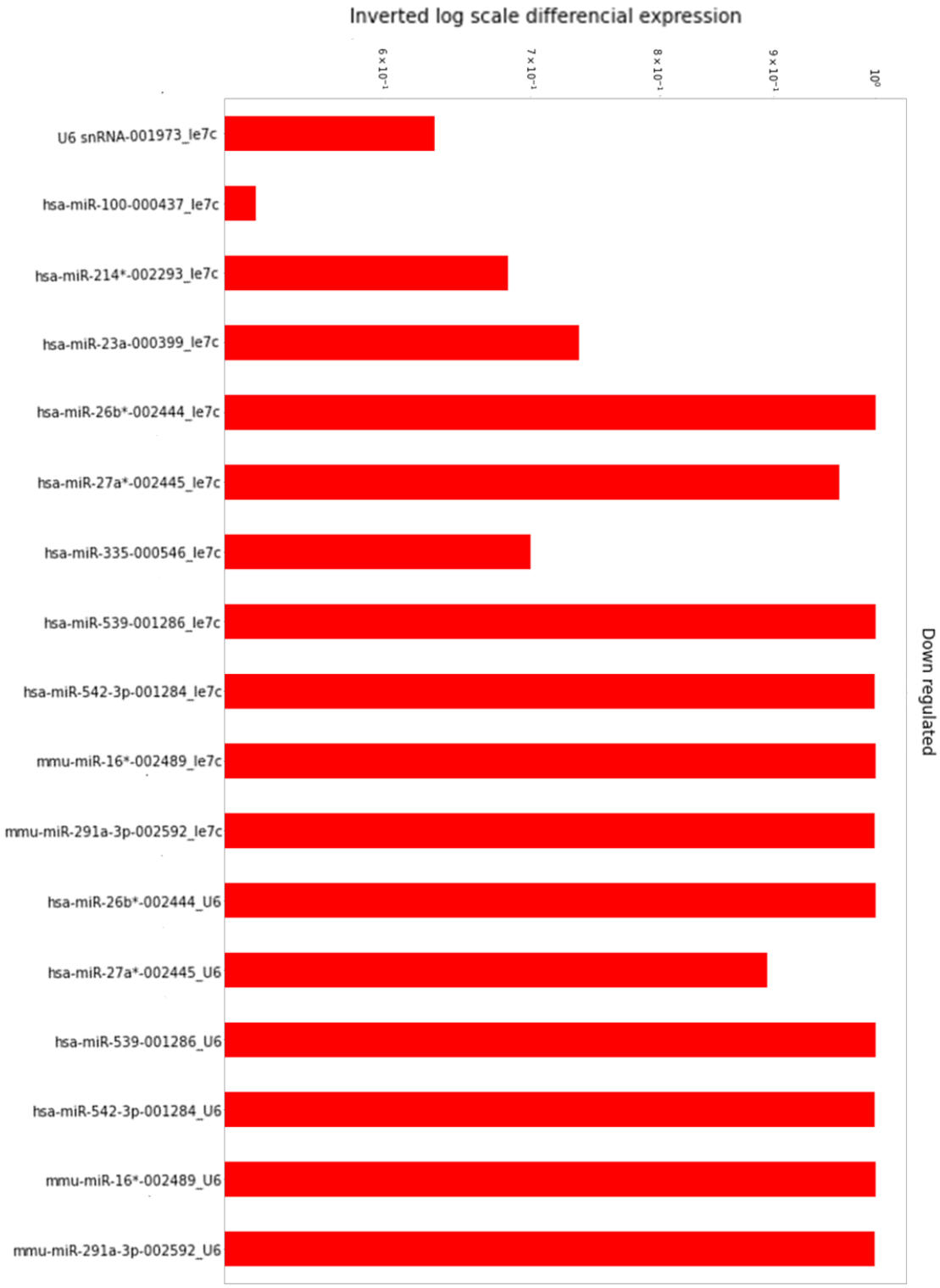

Figure 6. *Expression of down-regulated microRNAs in ovariectomized mice compared to Sham group. The expression levels are represented on an inverted logarithmic scale and normalized using let7 and U6 as endogenous controls.*

According to the cluster map and the correlation matrix, increased miR-31 levels are associated with a significant down-regulation of Wnt11 and a less significant one of Alpl and Crtap, whereas miR-199a overexpression is related to a significant down-regulation of Alpl and Crtap and a less significant one of Wnt11. A considerable over-expression of Dkk3 is correlated with the upregulation of miR-199a, which is also increased but less significantly in correlation with miR-31 (Figures 7, 8).

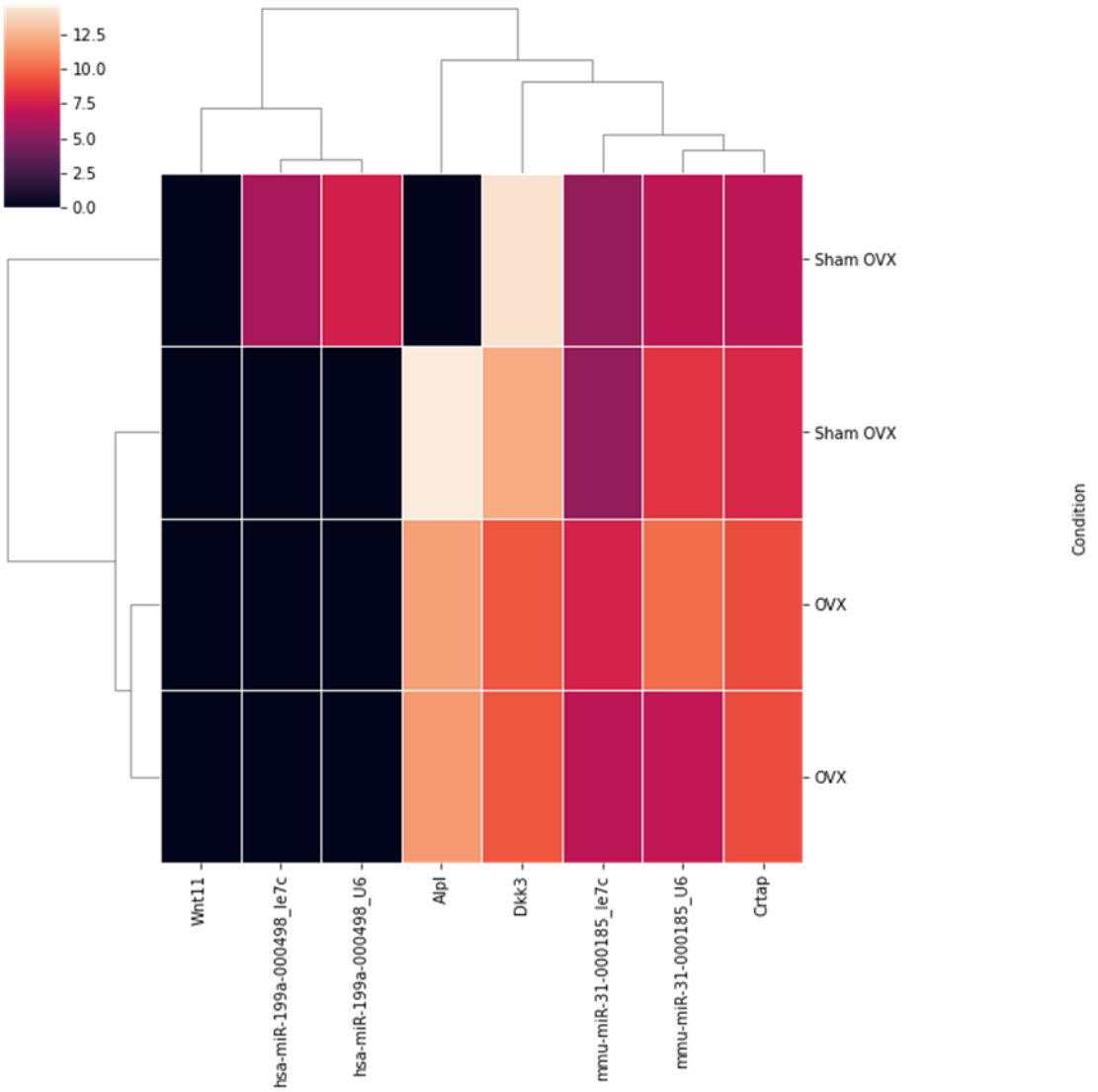

Figure 7. *Cluster map of highly supported up-regulated microRNAs and their correlated genes in ovariectomized mice compared to Sham group. The expression level values are referred to ΔCqs.*

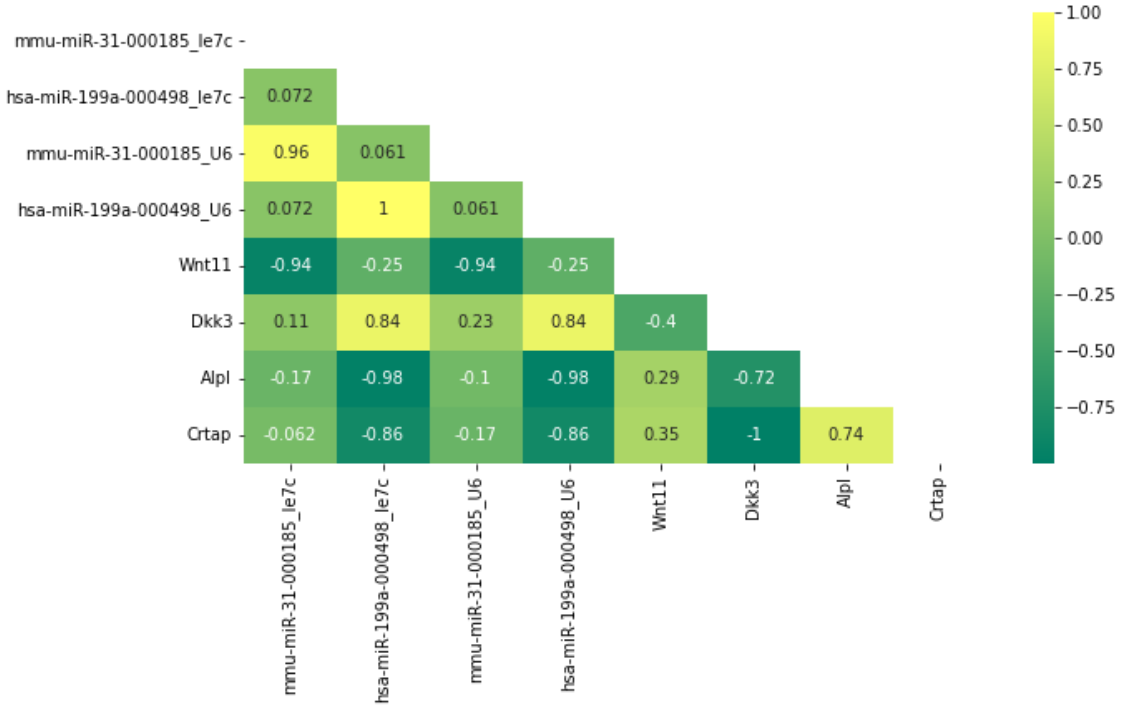

Figure 8. *Correlation matrix of highly supported up-regulated microRNAs and their correlated genes in ovariectomized mice compared to Sham group; values ranging from -0.8 to -1 indicating strong negative correlation, and values between 0.8 and 1 indicating strong positive correlation.*

In GIO mice, different clusters of differentially expressed microRNAs and their related genes were identified based on sex.

In particular, both miR-9 and miR-141* were highly upregulated in male GIO mice, followed by miR-346, miR-375, and miR-218 (Figure 9). Furthermore, the following miRNAs have been identified as being down-regulated: miR-27a*, miR-29a, miR-335, miR-31, miR-16*, let-7c, let-7d, let-7g, miR-100, miR-139-5p, miR-142-3p, miR-214*, miR-22, miR-23a, miR-26b*, miR-26b, miR-34a, miR-346, miR-374-5p (Figure 10).

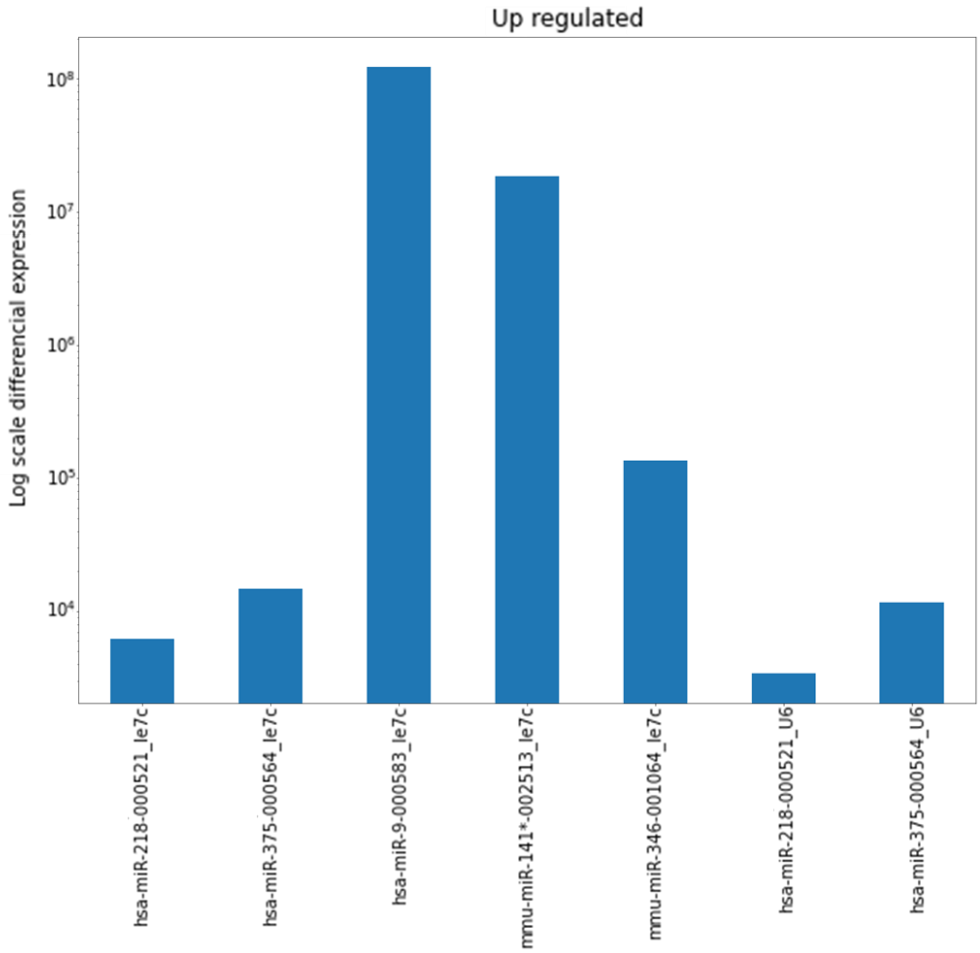

Figure 9. *Expression of up-regulated microRNAs in male GIO mice compared to Sham group. The expression levels are represented on a logarithmic scale and normalized using let7 and U6 as endogenous controls.*

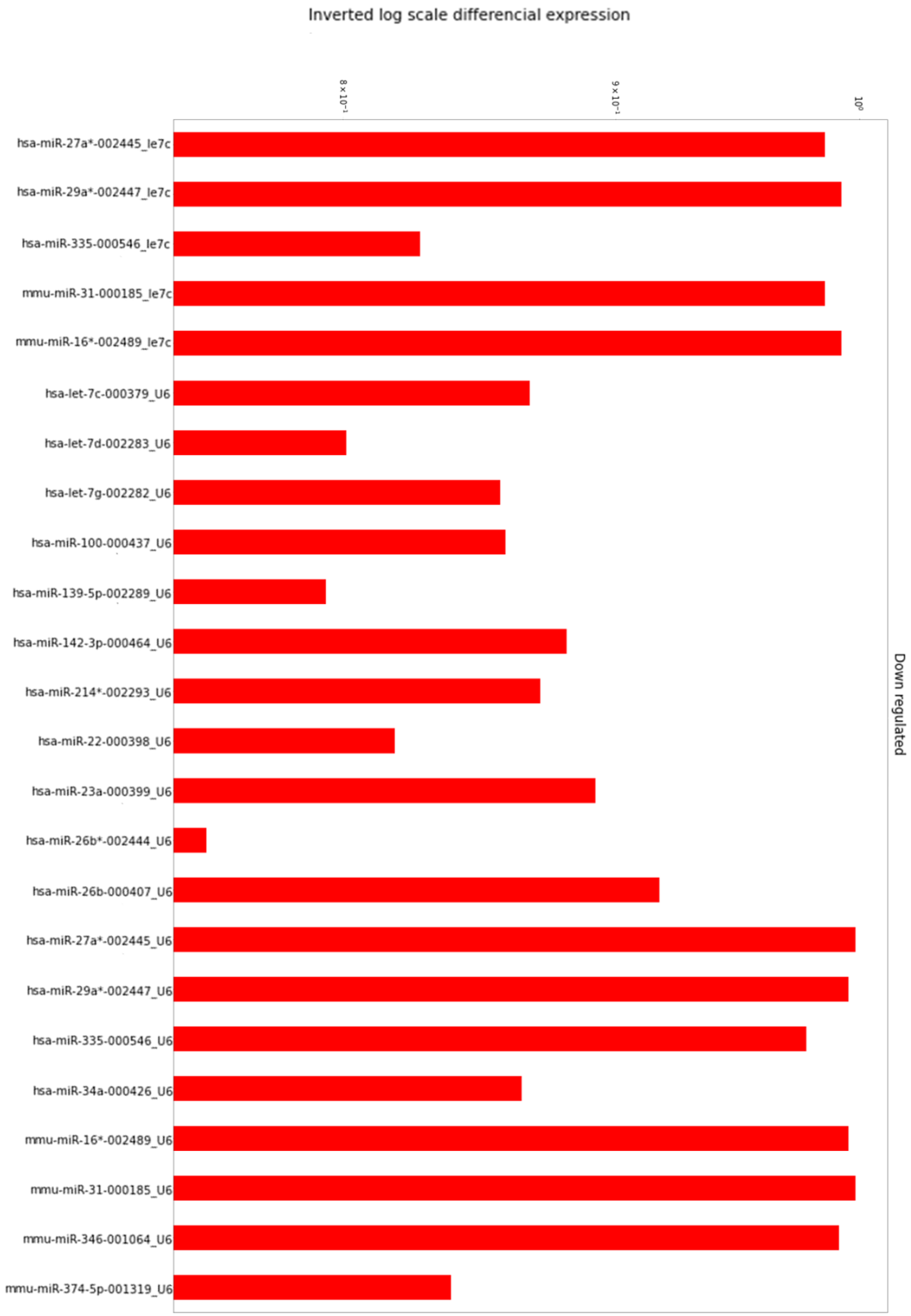

Figure 10. *Expression of down-regulated microRNAs in male GIO mice compared to Sham group. The expression levels are represented on an inverted logarithmic scale and normalized using let7 and U6 as endogenous controls.*

Additionally, the cluster map not only shows how male mice from the GIO group and those from the Sham group used for molecular investigations clustered perfectly, but, together with the correlation matrix, also reveals how the up-regulation of both miR-9 and miR-141* correlated to a strong down-regulation of Wnt5b, Wnt16, Ar, Pthr, and Alpl while, in contrast, to a significant overexpression of Apc, Csnk1a1, Dkk2, Dkk3, Mmp2 and Clcn7 (Figures 11, 12).

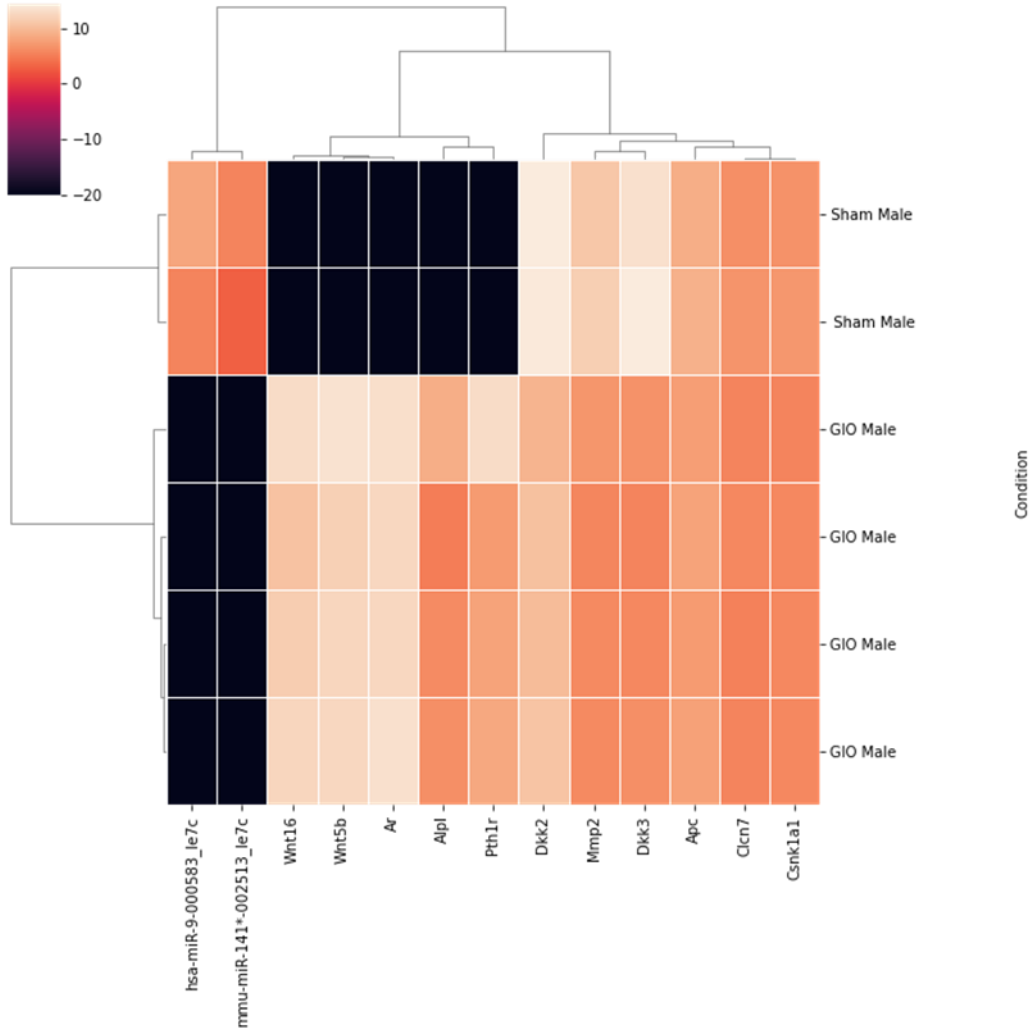

Figure 11. *Cluster map of highly supported up-regulated microRNAs and their correlated genes in male GIO mice compared to Sham group. The expression level values are referred to ΔCqs.*

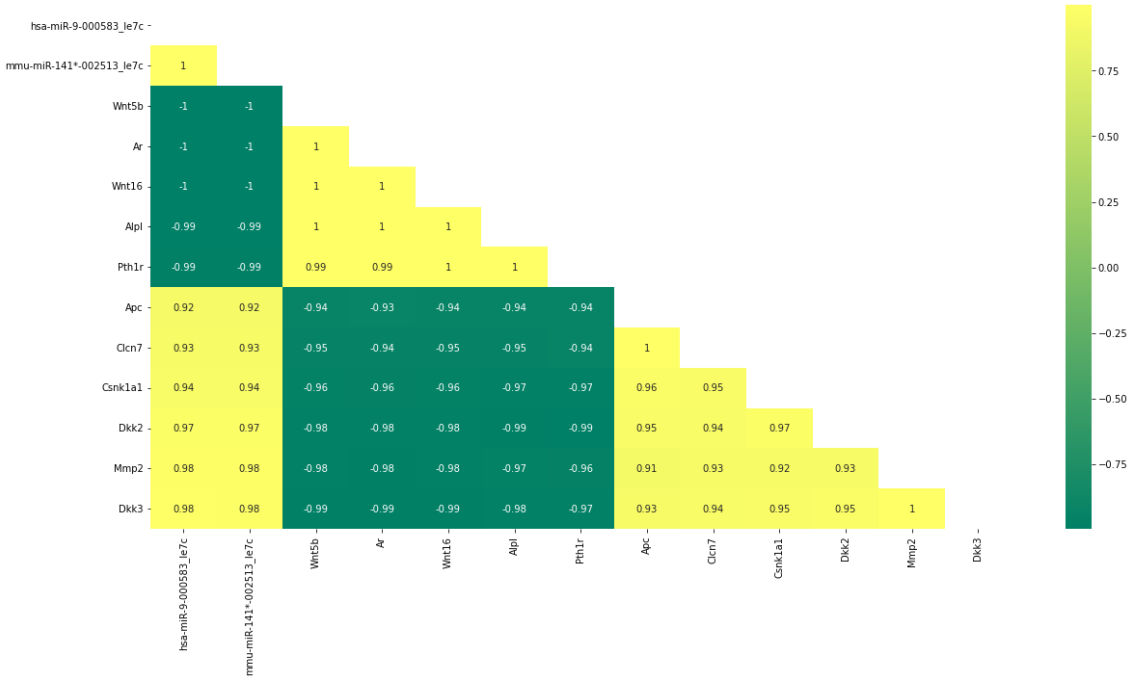

Figure 12. *Correlation matrix of highly supported up-regulated microRNAs and their correlated genes in male GIO mice compared to Sham group; values ranging from -0.8 to -1 indicating strong negative correlation, and values between 0.8 and 1 indicating strong positive correlation.*

Finally, let-7c was found to be highly upregulated in female GIO mice, followed by miR-542-3p (Figure 13), while let-7d, miR-100, miR-335, miR-34a, miR-374-5p, miR-375, miR-9, miR-16*, miR-291a-3p, miR-409-5p, miR-218, miR-26b*, miR-27a*, miR-539, miR-141*, miR-31, and miR-346 were observed to be down-regulated (Figure 14).

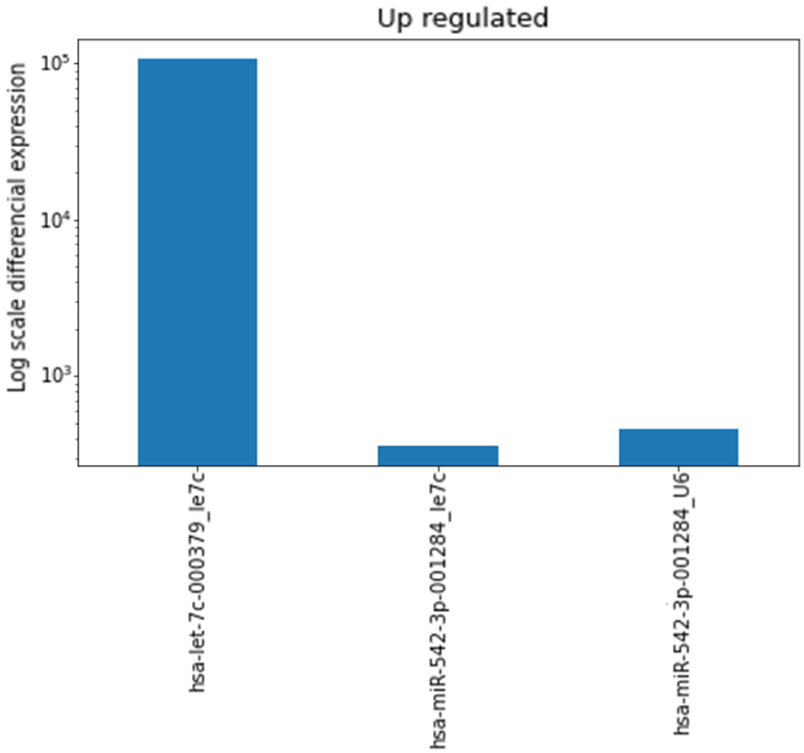

Figure 13. *Expression of up-regulated microRNAs in female GIO mice compared to Sham group. The expression levels are represented on a logarithmic scale and normalized using let7 and U6 as endogenous controls.*

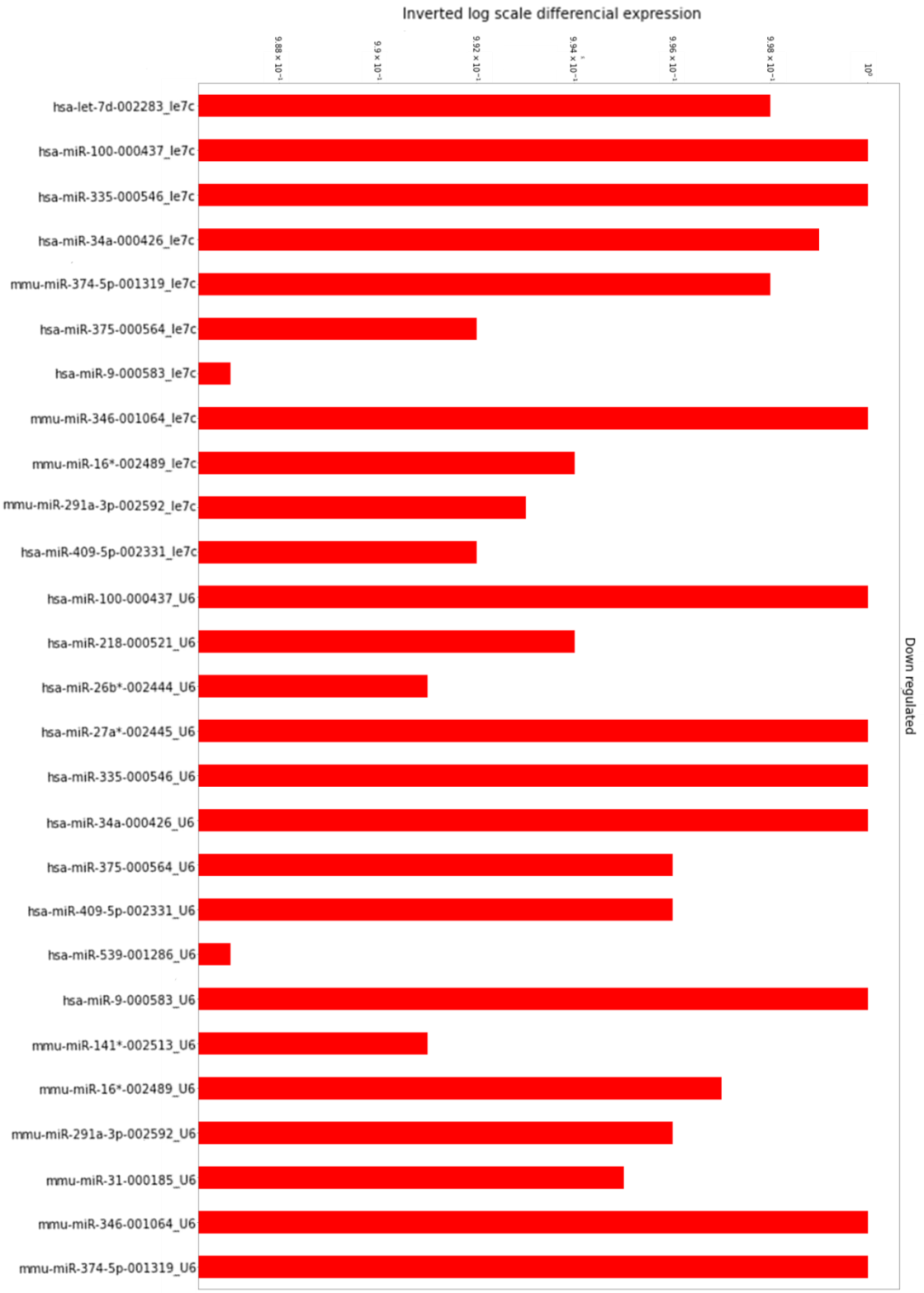

Figure 14. *Expression of down-regulated microRNAs in female GIO mice compared to Sham group. The expression levels are represented on an inverted logarithmic scale and normalized using let7 and U6 as endogenous controls.*

Based on let-7c and its related genes, the cluster map revealed that female GIO mice clustered perfectly with each other when compared to Sham mice (Figure 15). Moreover, according to the correlation matrix, overexpression of let-7c corresponded to a down-regulation of several genes involved in the Wnt pathway and bone formation, including: Fzd1, Fzd2, Fzd3, Fzd5, Fzd8, Wnt5a, Wnt5b, Wnt16, Lef1, Scd1, Ar, Pth1r, Igfbp2, Ccnd1, Pparg1a, Crtap, Bmp7, Col1a1, Col1a2, Bglap3 (Figure 16).

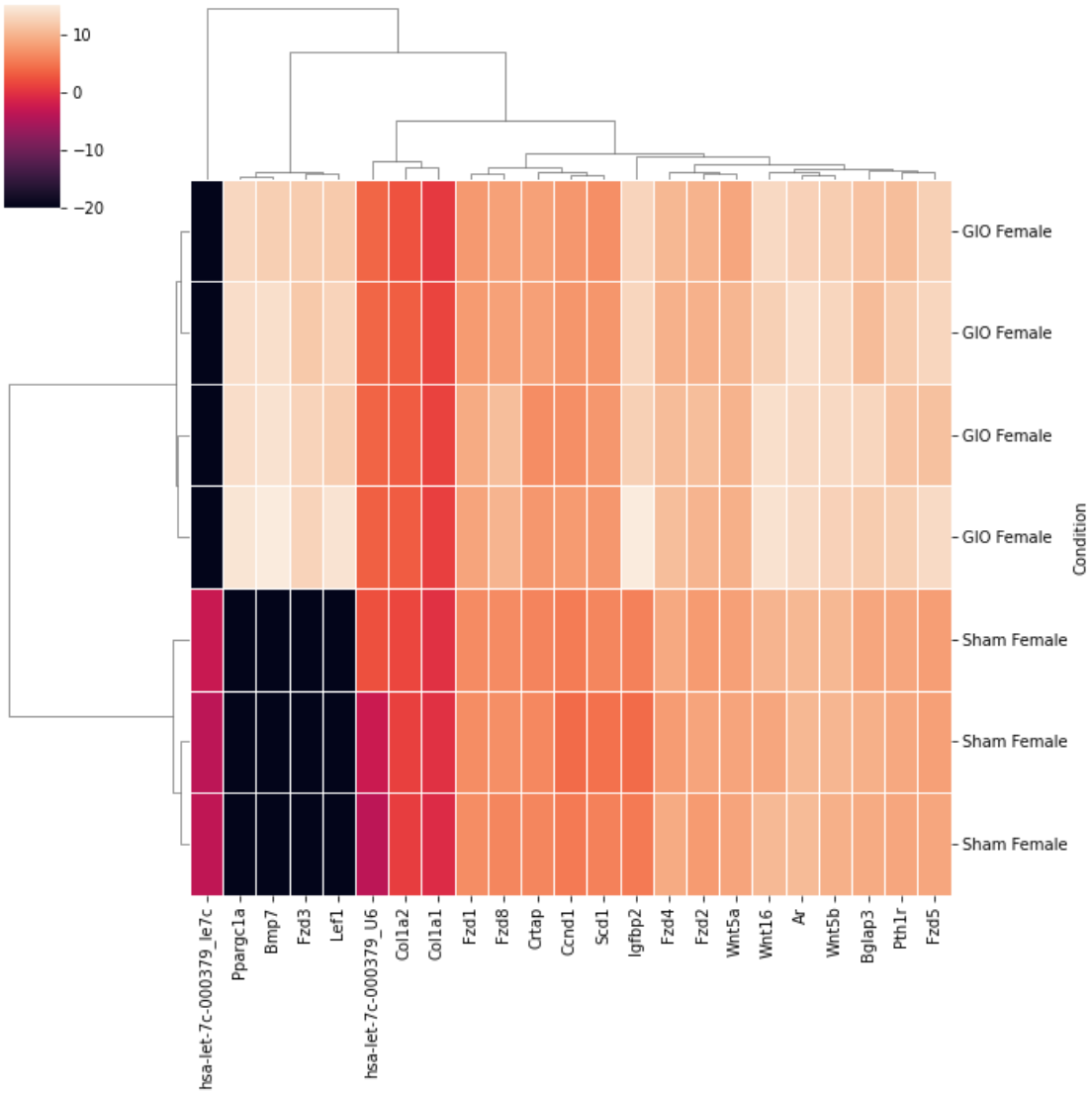

Figure 15. *Cluster map of highly supported up-regulated microRNAs and their correlated genes in female GIO mice compared to Sham group. The expression level values are referred to ΔCqs.*

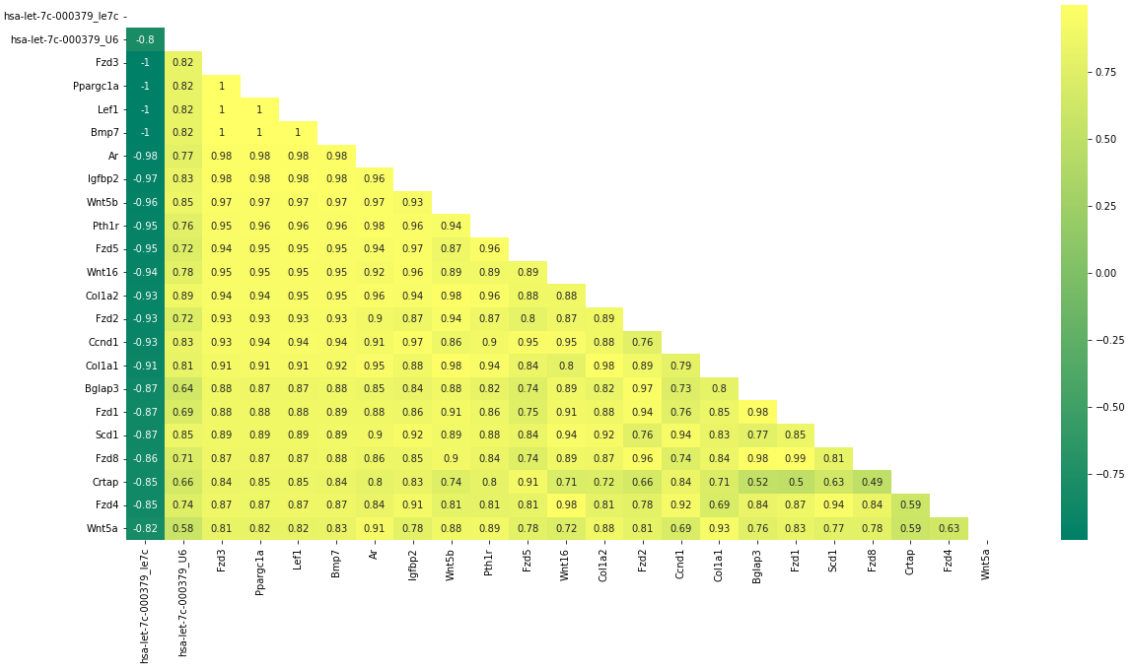

Figure 16. *Correlation matrix of highly supported up-regulated microRNAs and their correlated genes in female GIO mice compared to Sham group; values ranging from -0.8 to -1 indicating strong negative correlation, and values between 0.8 and 1 indicating strong positive correlation*

As a result of these findings, antagonists of miR-31 and miR-199a, miR-9 and miR-141*, and let-7c were chosen for the second phase of this research to treat ovariectomized mice, male GIO mice, and female GIO mice, respectively.

Administration of the assigned antagomirs stimulated osteogenesis in OVX and GIO mice osteoblasts.

The effect on bone homeostasis of the antagomirs assigned to each osteoporotic group was assessed by qPCR, evaluating the expression of genes involved in the early stages of osteoblastic differentiation: Runx2, BMP6, and Col1a1.

In the postmenopausal osteoporosis model, both Runx2, Bmp6, and Col1a1 (Figure 17 A, B, and C) appeared to be significantly down-regulated in untreated OVX mice and those given scramble compared to healthy controls, while in OVX treated with antagonists of miR-31-5p and miR-199a-5p, respectively, their expression, especially Runx2, was significantly increased compared to untreated or OVX given scramble.

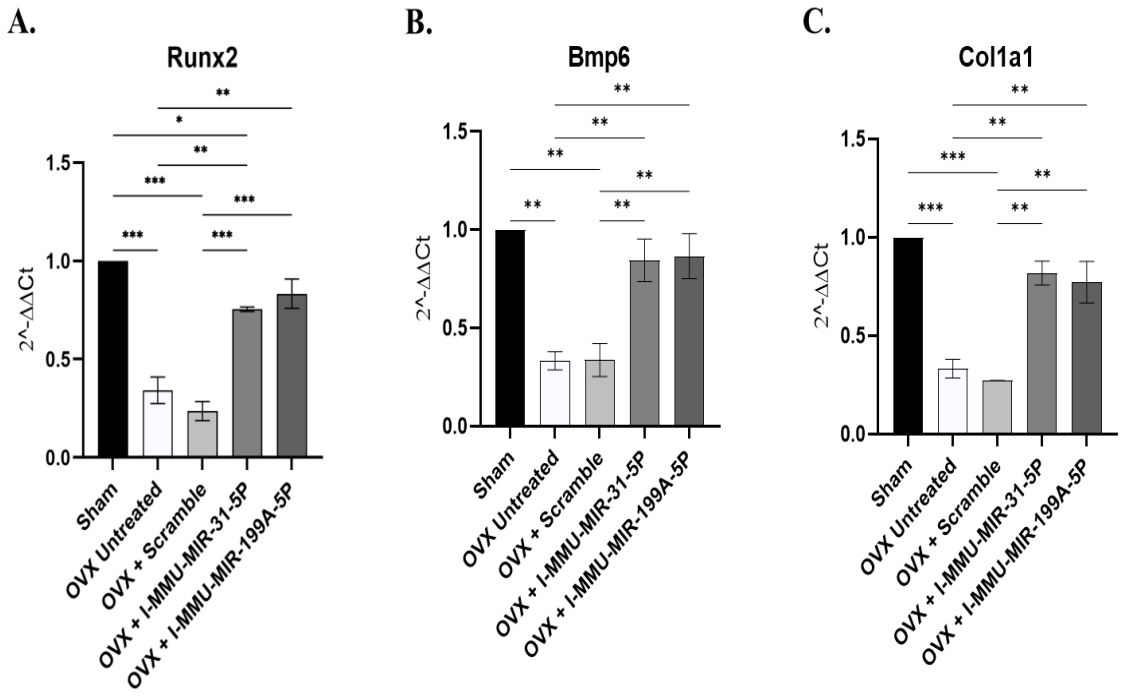

Figure 17. *qPCR results of (A) Runx2. (B) BMP6 (C) Col1a1 obtained from primary osteoblasts of: untreated OVX mice (OVX Untreated); OVX given scramble (OVX + Scramble); OVX administered with the antagonists of miR-31-5p (OVX + I-MMU-MIR-31-5P) and miR-199a (OVX + I-MMU-MIR-199A-5P), respectively. Sham group was used as negative control. Error bars correspond to standard error; *p < 0.05; **p < 0.01; *** p < 0.001, and ****p<0.0001.*

A similar situation was observed in the male GIO model, where the expression of Runx2, Bmp6, and Col1a1 (Figure 18 A, B, and C) was significantly reduced in untreated and

scramble-administered male GIO, while compared to them, it significantly increased in male GIO treated with the antagomir of miR-9-5p and miR-141-3p, respectively. However, even if Runx2, Bmp6, and Col1a1 were significantly more expressed in mice treated with anti-miR-9-5p than in GIO mice that did not receive antagomirs, they were still significantly less expressed than in healthy controls. On the other hand, anti-miR-141-3p did not show significant differences when compared to sham group for all of the three tested targets.

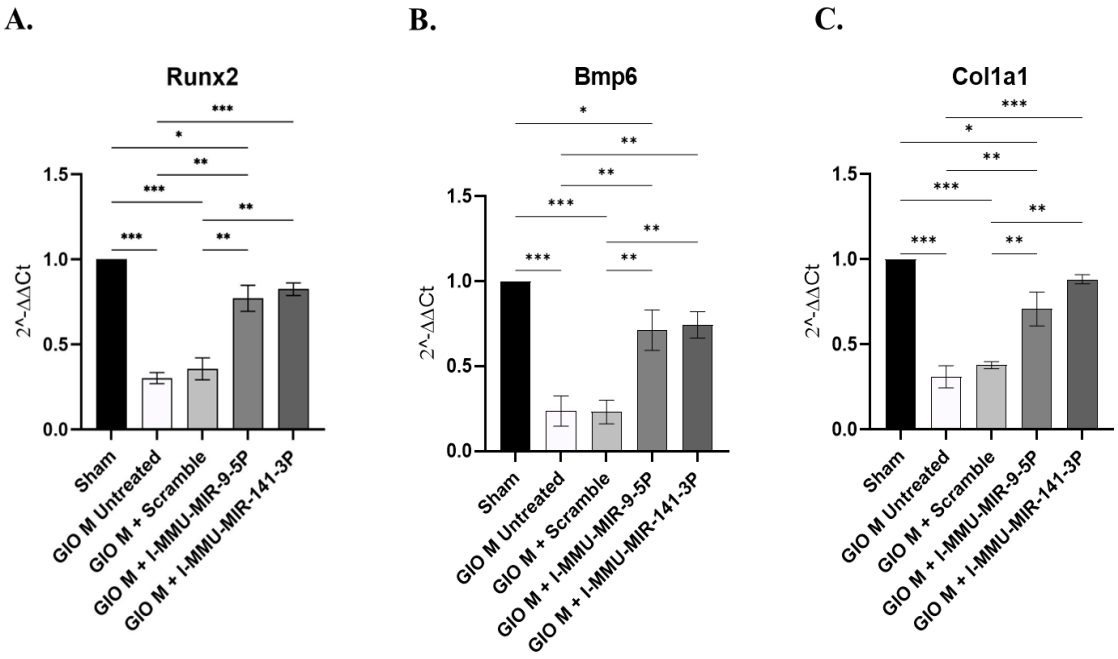

Figure 18. *qPCR results of (A) Runx2. (B) BMP6 (C) Col1a1 obtained from primary osteoblasts of: untreated male GIO mice (GIO M Untreated); male GIO given scramble (GIO M + Scramble); male GIO administered with the antagonists of miR-9-5p (GIO M + I-MMU-MIR-9-5P) and miR-141* (GIO M + I-MMU-MIR-141-3P), respectively. Sham group was used as negative control. Error bars correspond to standard error; *p < 0.05; **p < 0.01; *** p < 0.001, and ****p<0.0001.*

Finally, in the female GIO model, Runx2, Bmp6, and Col1a1 (Figure 19 A, B, and C) were up-regulated when compared to the respective untreated and scramble-administered GIO groups, although Runx2 was little significantly less up-regulated than in healthy controls.

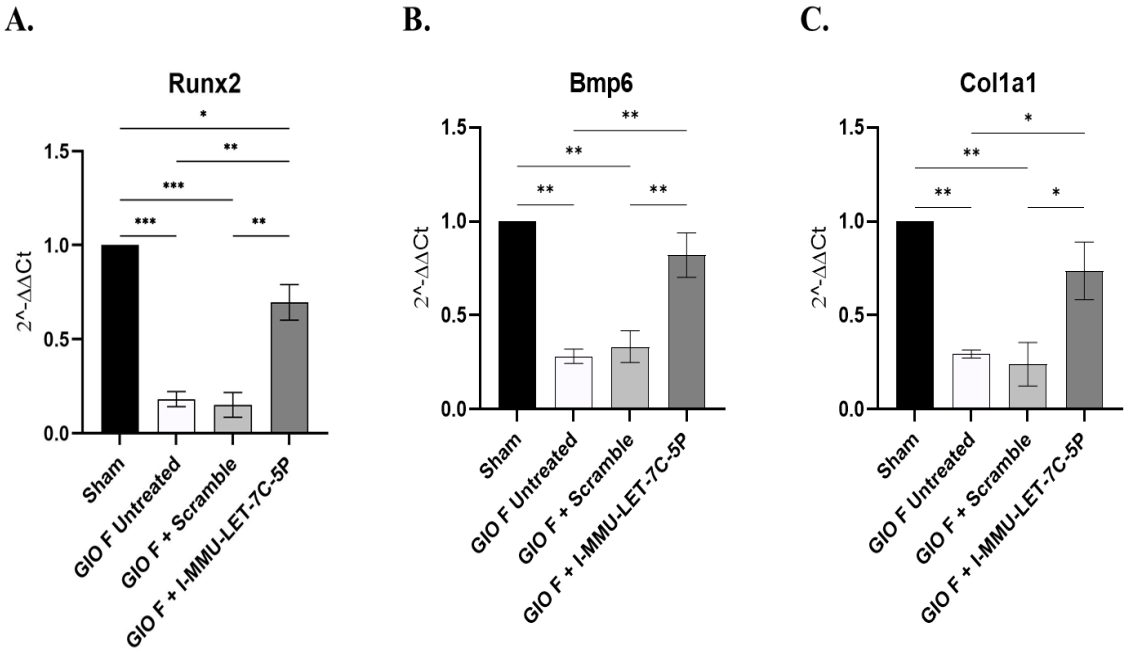

Figure 19. *qPCR results of (A) Runx2. (B) BMP6 (C) Col1a1 obtained from primary osteoblasts of: untreated female GIO mice (GIO F Untreated); female GIO given scramble (GIO F + Scramble); female GIO administered with the antagonist of let-7c-5p (GIO F + I-MMU-LET-7C-5P) and miR-141* (GIO M + I-MMU-MIR-141-3P), respectively. Sham group was used as negative control. Error bars correspond to standard error; *p < 0.05; **p < 0.01; *** p < 0.001, and ****p<0.0001.*

Treatment with designed antagomirs ameliorated bone architecture in osteoporotic mice.

The micro-CT axial images revealed that femurs of untreated (Figure 20 B) and scramble-treated OVX mice (Figure 20 C) exhibited a reduction in cortical and trabecular thickness,

as well as the presence of large pores indicative of osteoporotic state, compared to Sham group (Figure 20 A). On the other hand, the treatment with miR-31 (Figure 20 D) and miR-199a antagonists (Figure 20 E) improved the trabecular thickness in OVX mice femurs, while the quantity and size of pores was also reduced.

A.

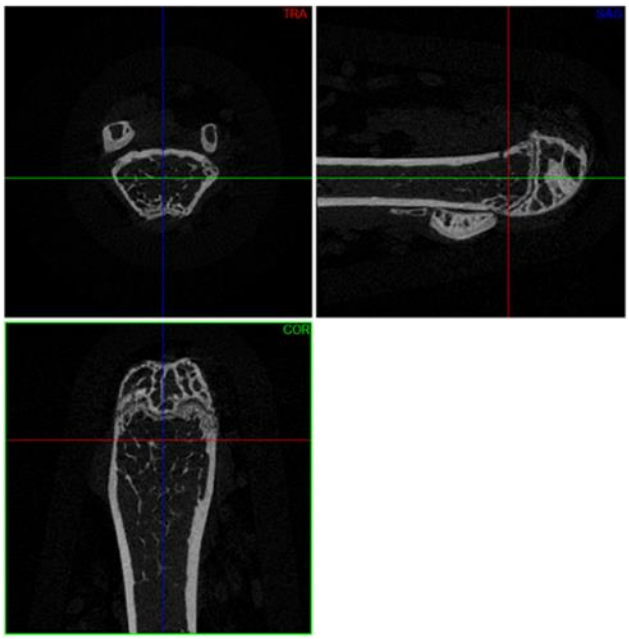

B.

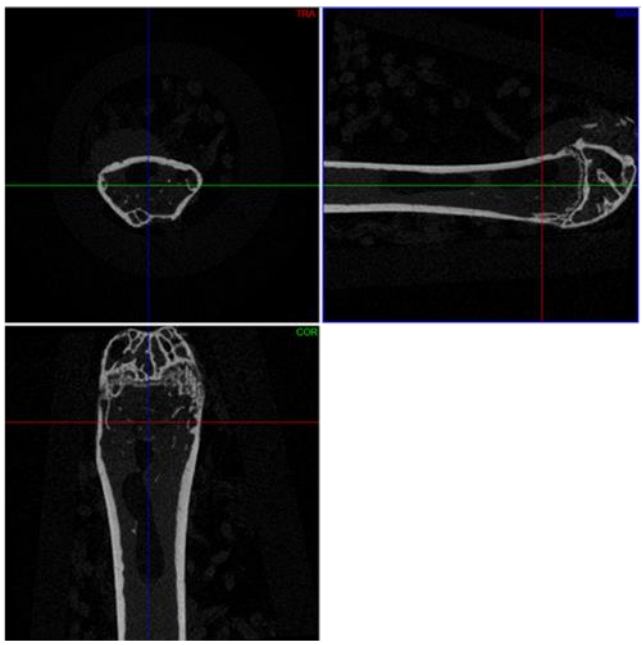

C.

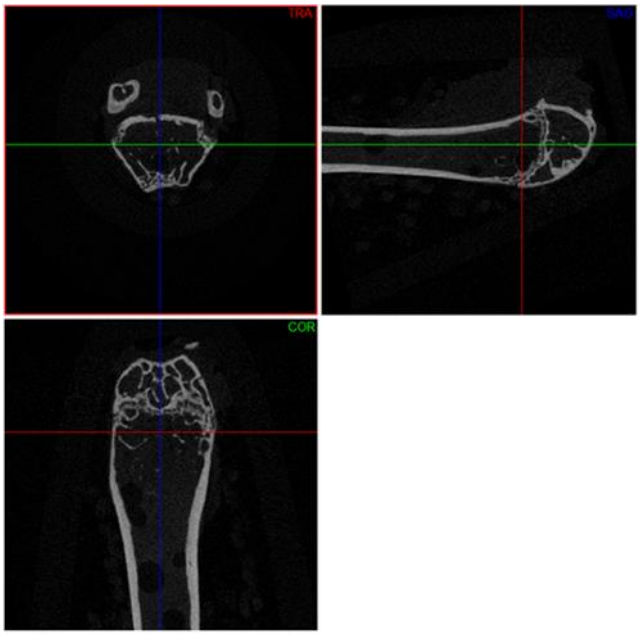

D.

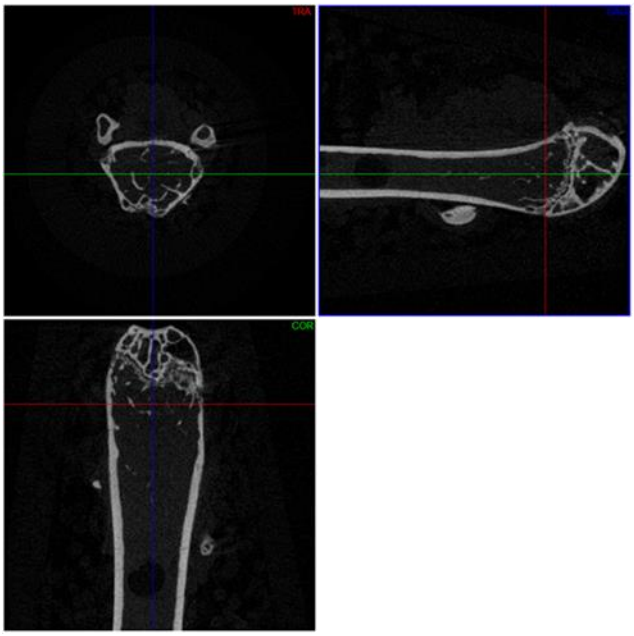

E.

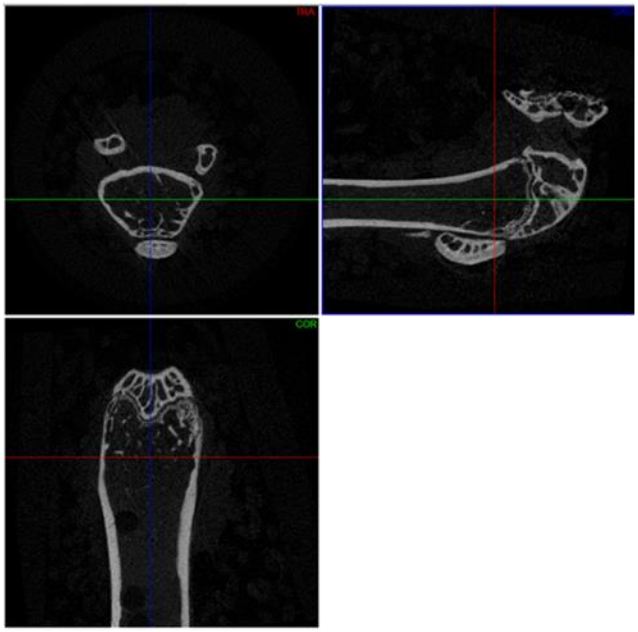

Figure 20. *Representative micro-CT axial images obtained from femoral distal epiphyses of each investigated group of OVX model. (A) Sham; (B) OVX untreated; (C) OVX + scramble; (D) OVX + I-MMU-MIR-31-5P; (E) OVX + I-MMU-MIR-199A-5P.*

In addition, the analysis of 3D micro-CT parameters of bone structure at femoral distal epiphysis confirmed that both untreated (BV/TV_{mean} 12,5%; $Tb.Th_{mean}$ 44,59 μm; Figure 21 B) and scramble-treated (BV/TV_{mean} 13,09%; $Tb.Th_{mean}$ 43,29 μm; Figure 21 C) OVX mice showed reduced trabecular thickness and bone fraction compared to Sham group (BV/TV_{mean} 15,95%; $Tb.Th_{mean}$ 56,22 μm; Figure 21 A), and to OVX mice treated with anti-miR-31 (BV/TV_{mean} 15,15%; $Tb.Th_{mean}$ 48,25 μm; Figure 21 D), and with anti-miR-199a (BV/TV_{mean} 14,08 %; $Tb.Th_{mean}$ 47,85 μm; Figure 21 E), where a recovery of trabecular microarchitecture and mineralization was observed.

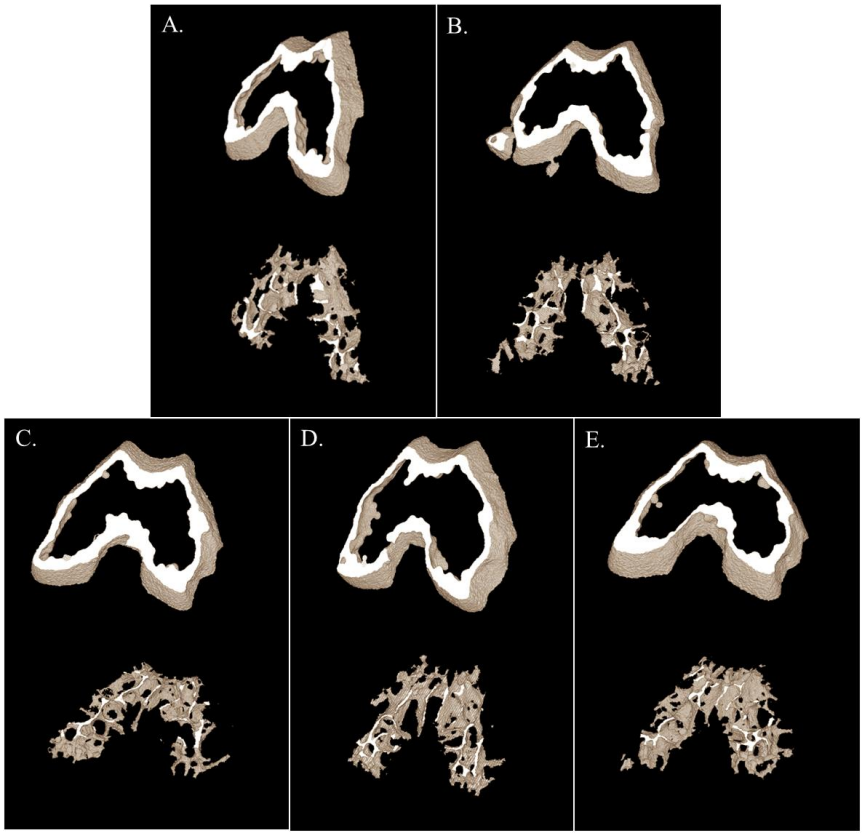

Figure 21. *Representative micro-CT three-dimensional images of cortical and trabecular bone microarchitecture obtained from femoral distal epiphyses of each investigated group of OVX model. (A) Sham; (B) OVX untreated; (C) OVX + scramble; (D) OVX + I-MMU-MIR-31-5P; (E) OVX + I-MMU-MIR-199A-5P.*

Femurs of untreated (Figure 22 B) and scramble-treated male GIO mice (Figure 22 C) showed a reduction in cortical and trabecular thickness, and an increased porosity compared to male Sham group (Figure 22 A). On the other hand, an increased thickness of trabeculae, and a reduced porosity were observed when male GIO mice were treated with anti-miR-9 (Figure 22 D), and anti-miR-141-3p (Figure 22 E), compared with the untreated ones.

A.

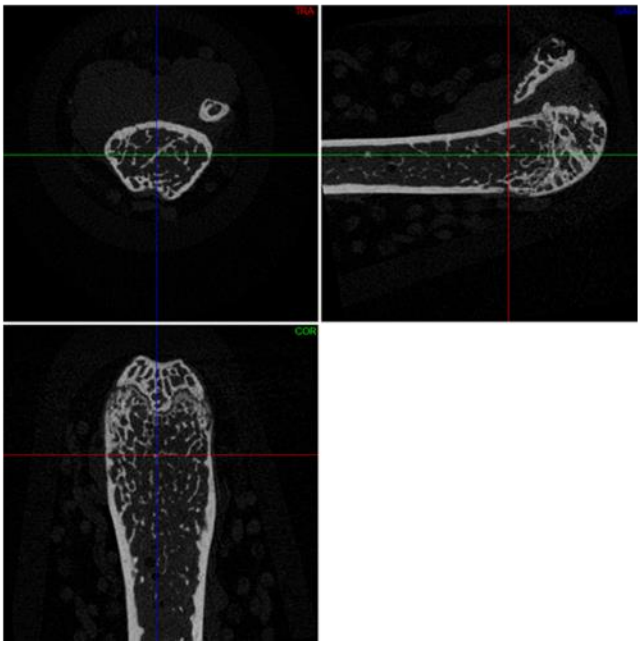

B.

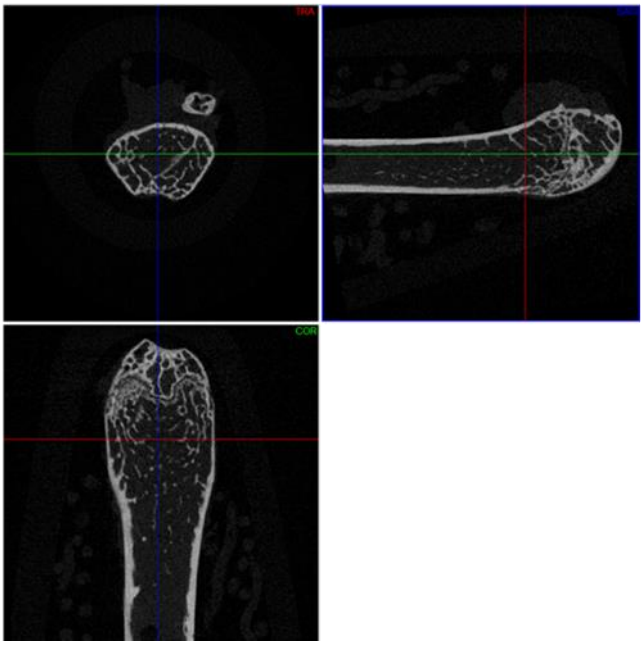

C.

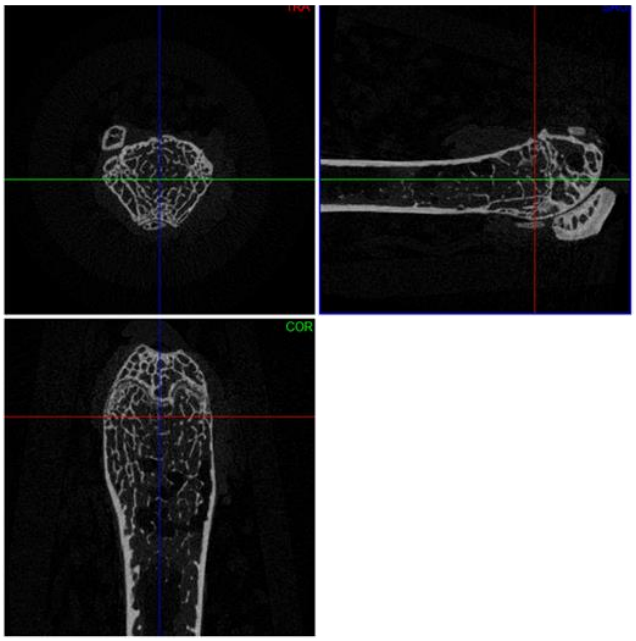

D.

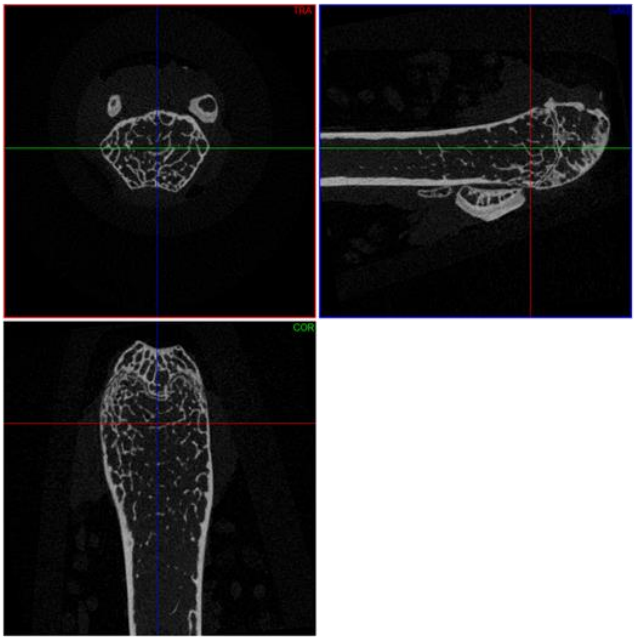

E.

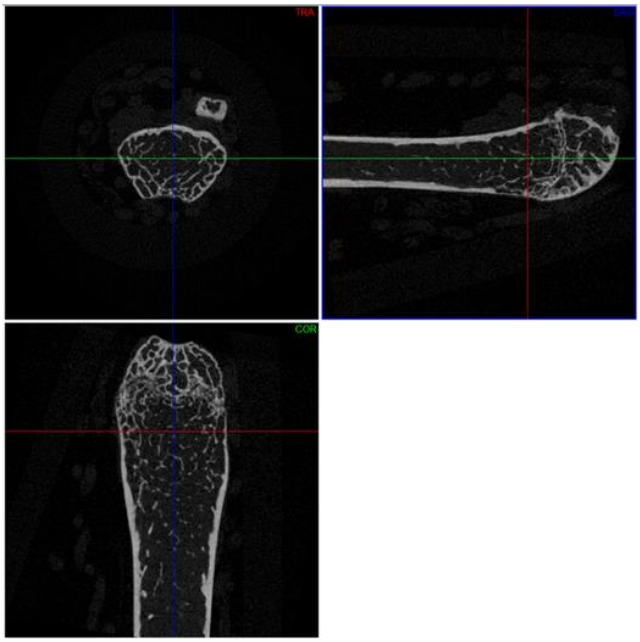

Figure 22. *Representative micro-CT axial images obtained from femoral distal epiphyses of each investigated group of male GIO model. (A) male Sham; (B) male GIO untreated; (C) male GIO + scramble; (D) male GIO + I-MMU-MIR-9-5P; (E) male GIO + I-MMU-MIR-141-3P.*

According to the 3D reconstruction analysis, a restoration of bone fraction and trabecular morphology was observed in male GIOs treated with anti-miR-9 (BV/TV_{mean} 20,21%; $Tb.Th_{mean}$ 45,31 μm; Figure 23 D) and anti-miR-141-3p (BV/TV_{mean} 18,99%; $Tb.Th_{mean}$ 45,69 μm; Figure 23 E), when compared to untreated (BV/TV_{mean} 15,91%; $Tb.Th_{mean}$ 40,85 μm; Figure 23 B) and scramble-treated ones (BV/TV_{mean} 17,44%; $Tb.Th_{mean}$ 42,15 μm; Figure 23 C), and with male Shams (BV/TV_{mean} 19,35%; $Tb.Th_{mean}$ 51,27 μm; Figure 23 A).

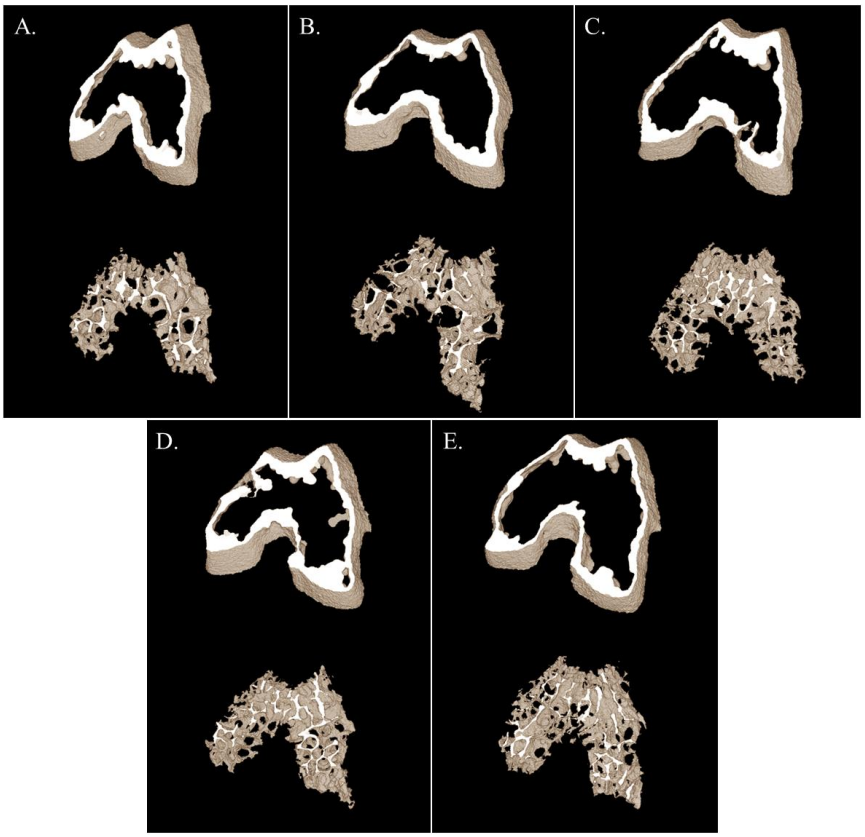

Figure 23. *Representative micro-CT three-dimensional images of cortical and trabecular bone microarchitecture obtained from femoral distal epiphyses of each investigated group of male GIO model. (A) male Sham; (B) male GIO untreated; (C) male GIO + scramble; (D) male GIO + I-MMU-MIR-9-5P; (E) male GIO + I-MMU-MIR-141-3P.*

Finally, compared to female Shams (Figure 24 A), cortical and trabecular thickness were found to be reduced in untreated female GIO mice (Figure 24 B) and in scramble-treated ones (Figure 24 C), which also showed an increased porosity. These osteoporotic signs appeared to be alleviated in female GIO mice when treated with anti-let-7c (Figure 24 D).

A.

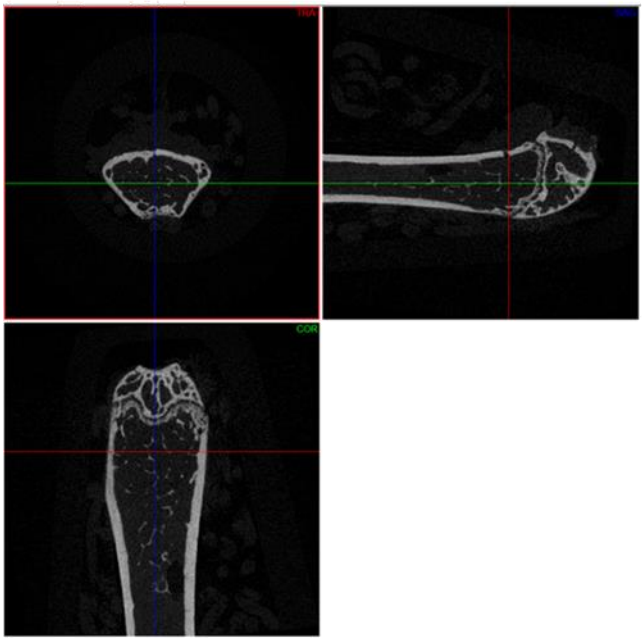

B.

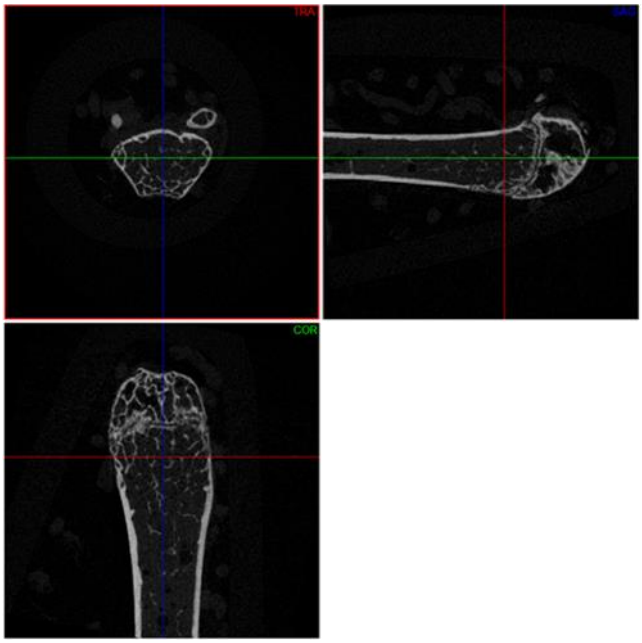

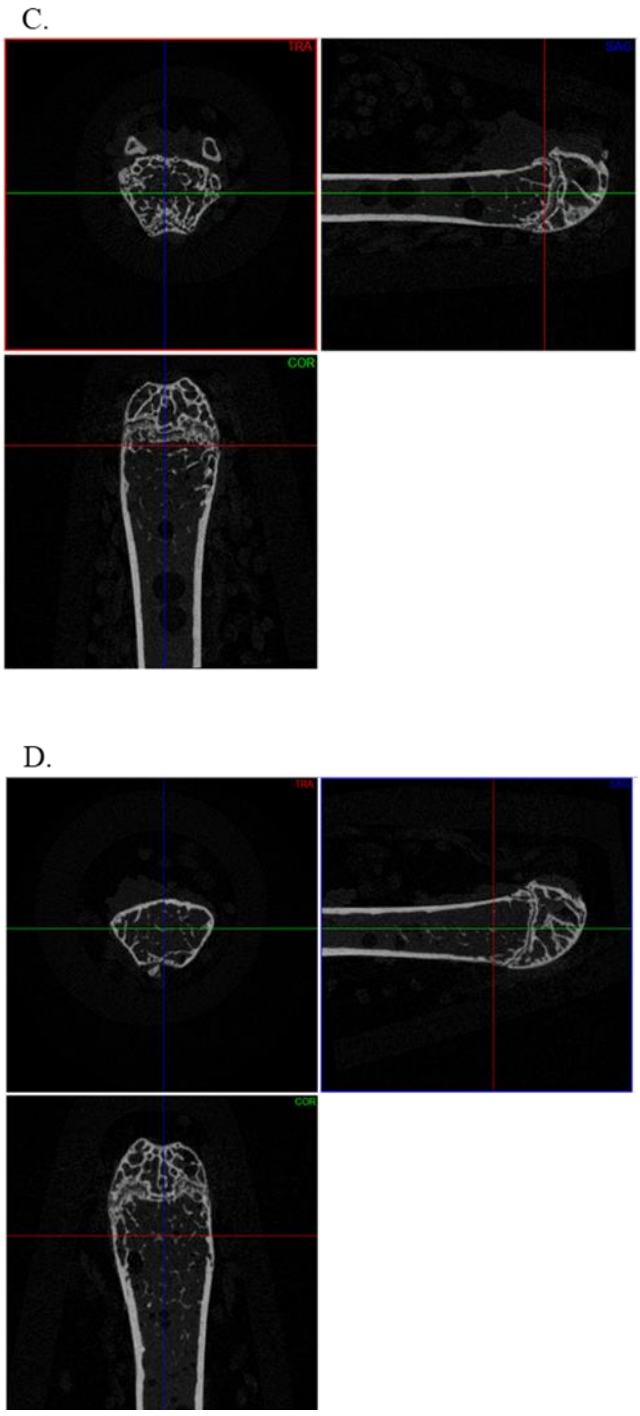

Figure 24. *Representative micro-CT axial images obtained from femoral distal epiphyses of each investigated group of female GIO model. (A) female Sham; (B) female GIO untreated; (C) female GIO + scramble; (D) female GIO + I-MMU-LET-7C-5P.*

Furthermore, morphometric 3D analysis revealed that female GIO mice treated with anti-let-7c (BV/TV_{mean} 16,5%; $Tb.Th_{mean}$ 48,93 μm; Figure 25 D) showed a repaired bone microarchitecture, comparing them to both female shams (BV/TV_{mean} 15,65%; $Tb.Th_{mean}$ 51,89 μm; Figure 25 A) and the untreated (BV/TV_{mean} 14,05%; $Tb.Th_{mean}$ 38,67 μm; Figure 25 B) or scramble-treated (BV/TV_{mean} 13,09%; $Tb.Th_{mean}$ 43,29 μm; Figure 25 C) female GIOs.

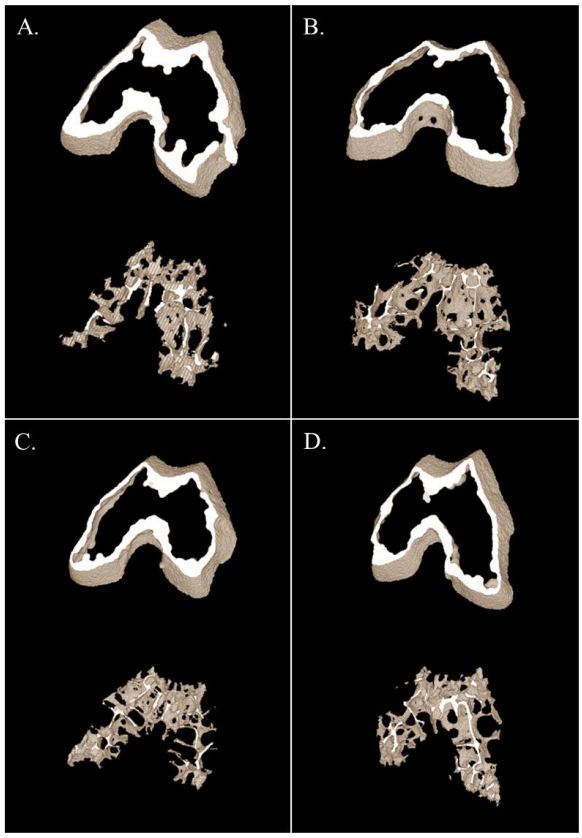

Figure 25. *Representative micro-CT three-dimensional images of cortical and trabecular bone microarchitecture obtained from femoral distal epiphyses of each investigated group of female GIO model. (A) female Sham; (B) female GIO untreated; (C) female GIO + scramble; (D) female GIO + I-MMU-LET-7C-5P.*

Treatment with antagomirs improved bone architecture and cellularity in OVX and GIO mice.

According to histological analysis of femur heads, both male and female Shams (Figure 26 A, and B) showed normal bone architecture and cellularity, which were not found in ovariectomized mice and in both male and female glucocorticoid-induced mice (Figure 26 C, D, and E), characterized by reduced cellularity and osteoporotic lesions. On the other hand, osteoporotic mice treated with the most representative antagomirs of each group (anti-miR-31 for OVX; anti-miR-141-3p for male GIOs; and anti-let-7c for female GIOs) (Figure 26 F, G, and H) showed signs of cellularity and bone architecture recovery, compared to the untreated ones.

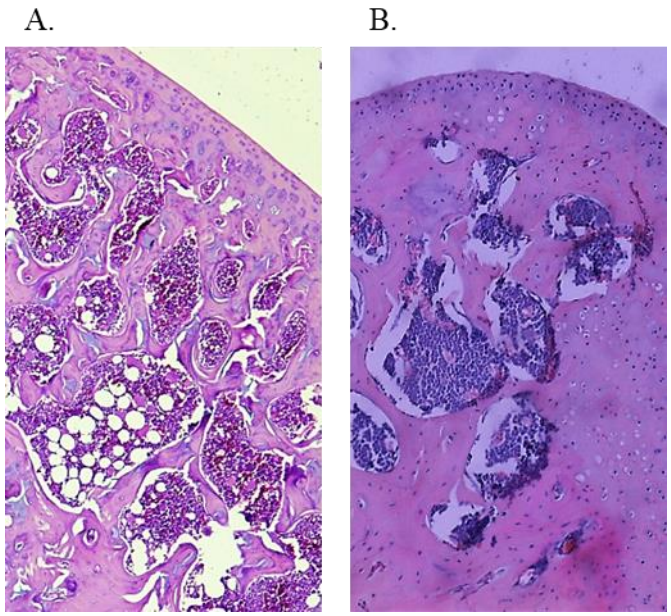

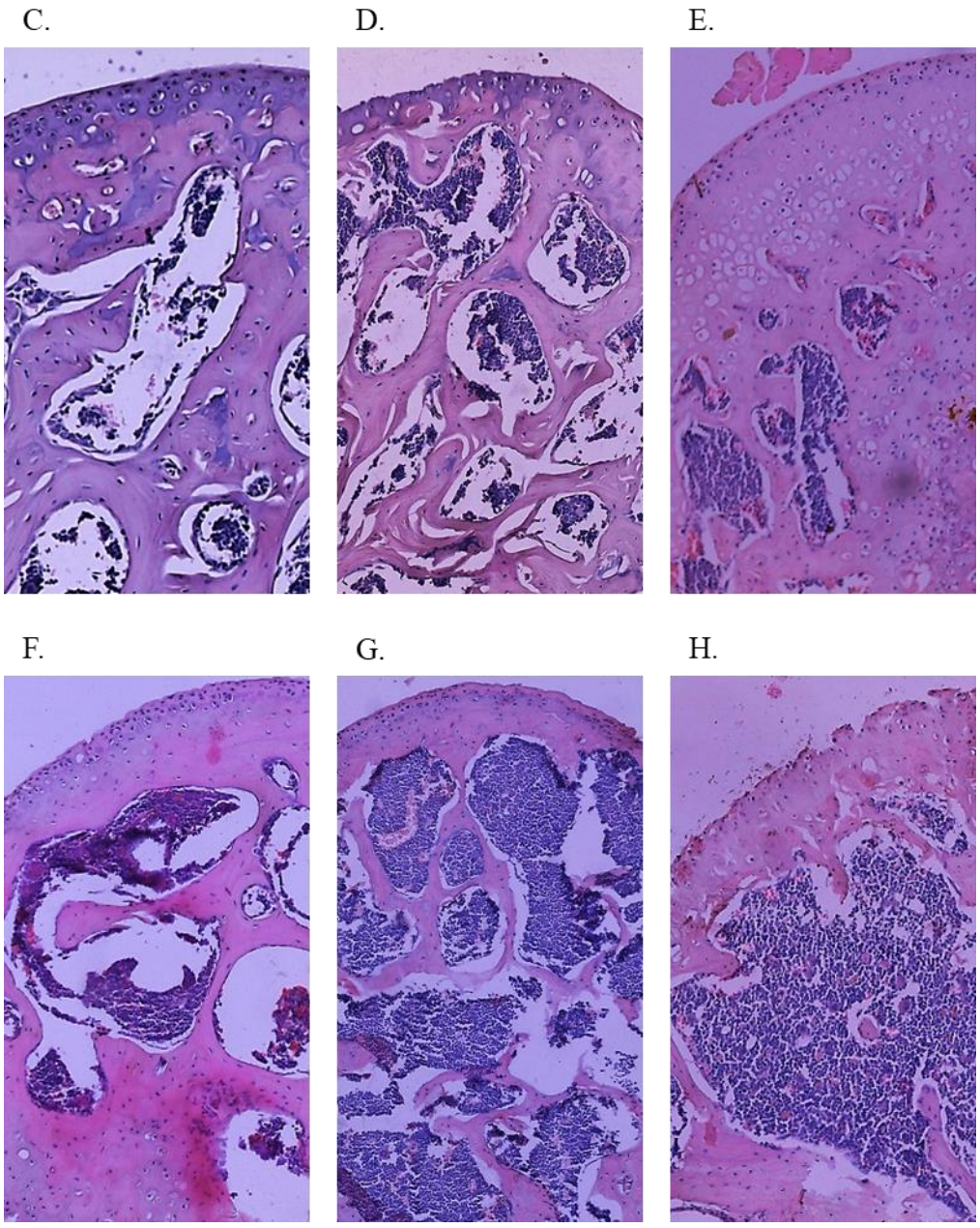

Figure 26. *Representative H&E staining of femur heads, 10X magnification. (A) female SHAM; (B) male SHAM; (C) OVX untreated; (D) male GIO untreated; (E) female GIO untreated; (F) OVX + I-MMU-MIR-31-5P; (G) male GIO + I-MMU-MIR-141-3P; (H) female GIO + I-MMU-LET-7C-5P.*

DISCUSSION

Population aging is a phenomenon that affects prevalence and incidence of osteoporosis, especially in Western Countries. As a consequence, it is clear that this condition represents a real public health emergency for both women and men, due to the significant economic and social costs, especially for the management of fragility fractures[141]. Many commonly prescribed medications also contribute to significant bone loss and fractures, including glucocorticoids, proton pump inhibitors (PPIs), selective serotonin receptor inhibitors (SSRIs), anticonvulsants, hormone deprivation therapy, calcineurin inhibitors, chemotherapies, and anticoagulants[142].

Osteoporotic fractures are frequently overlooked or misdiagnosed, resulting in severe disability or even death, more than other chronic noncommunicable diseases[143]. Therefore, best practices in prevention and treatment must be urgently investigated.

On the other hand, adherence to current osteoporosis medications is surprisingly low. In fact, approximately 20-30% of patients will discontinue treatment within 6 to 12 months of starting it, mainly due to socioeconomic factors, personal beliefs, healthcare system, and adverse drug effects, increasing their risk of osteoporotic fractures and hospitalization[144]. As a result, a valid therapeutic strategy for reversing both primary and secondary osteoporosis that is equally effective in women and men must be developed.

Furthermore, the majority of current osteoporosis treatments works to maintain the skeleton by only inhibiting bone resorption, while the introduction of new anabolic therapies that can increase bone formation and bone mass is of high relevance.

In this scenario, the Wnt pathway is known to induce osteoblast differentiation and suppress osteoclastic function, as well as being controlled by antagonists that directly interact with Wnt proteins or coreceptors. The evidence that several skeletal disorders are

associated with genetic alterations in Wnt pathway components emphasizes the importance of the Wnt signaling pathway to bone formation. As Wnt signaling promotes bone formation, blocking Wnt can decrease the skeletal anabolic response. Thus, advances in therapeutic approaches targeting Wnt antagonists to improve bone formation are also explored[145]. Some microRNAs can also be considered antagonists of the Wnt pathway, as they have been shown to be epigenetic regulators that inhibit Wnt effectors, thereby affecting bone metabolism[146].

Hence, exploiting microRNAs which affect Wnt signal as purported therapeutic targets for the treatment of osteoporosis could be a great chance. Within this regard, numerous studies have found that miRNA-based antagonism is effective in maintaining bone homeostasis. One major advantage of using miRNA-based drugs as is that the nucleotide content of the miRNAs can be easily modified by chemicals to improve their pharmacokinetics and pharmacodynamics. Moreover, chemical locked nucleic acid modifications prevent miRNA susceptibility to intracellular nucleases. Similarly, phosphorothioate modification is another method for increasing the efficacy of miRNAs in in vivo systems[147].

In the first phase of this study, several down-regulated miRNAs supported by the literature were identified in the two osteoporosis models under study. In particular, miR-27a-3p, miR-291a, and miR-335 were found to be down-regulated both in OVX mice and in male and female GIO mice. These are followed by: miR-539, which was down-regulated in both OVX mice and female GIOs; miR-346, whose expression was decreased in both sexes of GIO mice; miR-542, which revealed a reduced expression only in OVX mice; miR-29a-3p, miR-142-3p and miR-26b, which were down-regulated only in male GIOs; and miR-218 which was found to be reduced only in female GIOs. Indeed, several studies have shown that these microRNAs interfere with the Wnt signal by targeting Wnt

inhibitors or components of the β-catenin destruction complex, and that their down-regulation negatively affects bone homeostasis.

On the other hand, some miRNAs involved in the Wnt pathway were identified as potential therapeutic targets for osteoporosis treatment through the use of antagomirs: miR-31 and miR-199a in the postmenopausal osteoporosis model, while in the glucocorticoid-induced osteoporosis model miR-9 and miR-141-3p in males and let-7c in females were found to be up-regulated.

Besides being supported by the scientific literature, these up-regulated microRNAs have also been shown to correlate with genes involved in the Wnt pathway as well as bone homeostasis.

In ovariectomized mice, the up-regulation of miR-31 and miR-199a corresponded to a down-regulation of Wnt11 and Alpl. In this regard, several studies have shown that Wnt11 overexpression in pre-osteoblasts promote bone morphogenetic protein (BMP)-induced expression of alkaline phosphatase and mineralization by activating the canonical Wnt pathway[148,149]. Crtap, whose deficiency causes osteogenesis imperfecta[150], were also down-regulated, in contrast to Dkk3, an antagonist of the Wnt signal, which was found to be over-expressed. Based on these results, while the role of miR-31-5p appears controversial, considering that the prediction tool miRDB (mirdb.org) shows Dkk1 as its prediction target, miR-199a-5p predicted targets are instead represented by Wnt2, Wnt7a and Wnt9b, thus confirming its negative action in the canonical Wnt pathway.

In male GIO mice the up-regulation of both miR-9 and miR-141* was related to a strong down-regulation of Wnt5b and Wnt16, both of which promote osteogenesis through non-canonical Wnt pathways[151]. At the same time, the osteogenic marker Alpl, as well as the Ar and PTH1R receptors, which are also osteogenic promoters[152,153], were found to be

down-regulated, while Apc and Casein kinase 1α (Csnk1a1), which are components of the β-catenin destruction complex. In this regard, both miRNAs both miRNAs appear to have β-catenin as a predicted target. In addition, the Wnt antagonists Dkk2 and Dkk3, and Clcn7 and Mmp2, both of which are considered osteogenic inhibitors[154,155], were also found to be up-regulated. These data suggest that miR-9-5p and miR-141-3p could affect bone metabolism by interfering with both canonical and non-canonical Wnt cascades and probably generating a cross-talk between Wnt signal and both androgen and parathormone receptors, even if the mechanism is still not clear.

In female GIO mice, the increase in let-7c expression also corresponded to a down-regulation of Wnt5b, Wnt16, Ar and PTH1R. Among these down-regulated targets there were also included: Wnt5a, which, like Wnt5b, is known to promotes osteogenesis; Lef1, transcription factor of the canonical Wnt pathway; Scd1, a Wnt signal activator; the majority of Frizzled receptors, including Fzd1, Fzd2, Fzd3, Fzd5 and Fzd8; the osteogenic markers Bmp7, Col1a1, Col1a2, and Osteocalcin (Bglap3); Igfbp2 and PGC1α (Pparg1a), which are reported to induce osteoblastic differentiation[156,157]; Cyclin D1 (Ccnd1), which was found to be targeted by PTH and its related proteins (PTHrPs) to induce proliferative effects in early osteoblastic cells[158], and Crtap. In particular, two of the founded down-regulated genes appear to be predicted targets of let-7c: Fzd3, and Col1a2. This association suggests a greater involvement of the canonical Wnt pathway and a greater reduction of bone mineralization in female GIOs compared to males, considering that glucocorticoids are known to inhibit estrogenic responses [159], thus aggravating the osteoporotic condition more in women than in men.

To support these data, studies have shown that, while Wnt11 is not upregulated in ovariectomized mice or in mice treated with estradiol antagonists[160] since its expression

is induced by estrogen-related receptor alpha[161], glucocorticoids inhibit Wnt16 expression in osteoblasts, suppressing bone formation[162].

Hence, these findings suggest that those miRNAs that were found to be up-regulated in the two osteoporotic models could play a crucial role in bone remodeling by affecting the Wnt pathway and, therefore, the relative antagonists were selected for the next part of this research, which consisted in treating osteoporotic mice with the predicted antagomirs.

The results obtained from the second part of this study demonstrated how treatment with the designated antagomirs stimulated gene expression of markers involved in the osteogenic process in both ovariectomized and glucocorticoid-induced osteoporotic mice. These molecular findings were supported by microcomputed tomography and histological evaluations, which revealed that cortical and trabecular thickness, mineralization, porosity, as well as lesions and reduced cellularity found in OVX and GIO mice, appeared mitigated in animals treated with the assigned antagomirs.

CONCLUSIONS

In conclusion, these data suggest that treatment with miR-31-5p and miR-199a-5p antagonists in postmenopausal osteoporosis, and, respectively, anti-miR-9-5p and anti-miR-141-3p in men, and let-7c-5p antagomir in women with glucocorticoid-induced osteoporosis could be a valid anabolic therapeutic strategy that, compared to currently available drugs, could overcome the problem of toxicity and adverse side effects, as well as promote an increase in bone mass through the pro-osteogenic effect due to the modulation of the Wnt pathway. This would allow greater adherence to therapy by both women and men osteoporotic patients, as well as an improvement in their quality of life.

Further investigations will be required to identify the actual mRNAs involved in the Wnt signal that are directly targeted by the miRNAs that have been antagonized in this study, and to assess whether the use of these antagomirs could positively or negatively interfere with other physiological pathways. Therefore, future studies to identify other promising therapeutic approaches for the treatment of primary and secondary osteoporosis may also focus on the use of mimics to replace the regulatory effect of the aforementioned down-regulated miRNAs found in this study and implicated in Wnt signal.

REFERENCES

1. Glaser DL, Kaplan FS. Osteoporosis: Definition and Clinical Presentation. *Spine*. 1997;22(24):12S.

2. Lane NE. Epidemiology, etiology, and diagnosis of osteoporosis. *Am J Obstet Gynecol*. 2006;194(2):S3-S11. doi:10.1016/j.ajog.2005.08.047

3. Eriksen EF. Cellular mechanisms of bone remodeling. *Rev Endocr Metab Disord*. 2010;11(4):219-227. doi:10.1007/s11154-010-9153-1

4. Nakashima K, Zhou X, Kunkel G, et al. The novel zinc finger-containing transcription factor osterix is required for osteoblast differentiation and bone formation. *Cell*. 2002;108(1):17-29. doi:10.1016/s0092-8674(01)00622-5

5. Qin L, Qiu P, Wang L, et al. Gene expression profiles and transcription factors involved in parathyroid hormone signaling in osteoblasts revealed by microarray and bioinformatics. *J Biol Chem*. 2003;278(22):19723-19731. doi:10.1074/jbc.M212226200

6. Westendorf JJ, Kahler RA, Schroeder TM. Wnt signaling in osteoblasts and bone diseases. *Gene*. 2004;341:19-39. doi:10.1016/j.gene.2004.06.044

7. Huang W, Yang S, Shao J, Li YP. Signaling and transcriptional regulation in osteoblast commitment and differentiation. *Front Biosci J Virtual Libr*. 2007;12:3068-3092.

8. Bonewald L. Osteocytes as multifunctional cells. *J Musculoskelet Neuronal Interact*. 2006;6(4):331-333.

9. Fitzpatrick LA. Secondary Causes of Osteoporosis. *Mayo Clin Proc*. 2002;77(5):453-468. doi:10.4065/77.5.453

10. Waters KM, Rickard DJ, Riggs BL, et al. Estrogen regulation of human osteoblast function is determined by the stage of differentiation and the estrogen receptor isoform. *J Cell Biochem*. 2001;83(3):448-462. doi:10.1002/jcb.1242

11. Li L, Wang Z. Ovarian Aging and Osteoporosis. In: Wang Z, ed. *Aging and Aging-Related Diseases: Mechanisms and Interventions*. Advances in Experimental Medicine and Biology. Springer; 2018:199-215. doi:10.1007/978-981-13-1117-8_13

12. Compston J. Glucocorticoid-induced osteoporosis: an update. *Endocrine*. 2018;61(1):7-16. doi:10.1007/s12020-018-1588-2

13. Wu Z, Bucher NL, Farmer SR. Induction of peroxisome proliferator-activated receptor gamma during the conversion of 3T3 fibroblasts into adipocytes is mediated by C/EBPbeta, C/EBPdelta, and glucocorticoids. *Mol Cell Biol*. 1996;16(8):4128-4136. doi:10.1128/MCB.16.8.4128

14. Sato AY, Cregor M, Delgado-Calle J, et al. Protection From Glucocorticoid-Induced Osteoporosis by Anti-Catabolic Signaling in the Absence of Sost/Sclerostin. *J Bone Miner Res Off J Am Soc Bone Miner Res*. 2016;31(10):1791-1802. doi:10.1002/jbmr.2869

15. Ohnaka K, Tanabe M, Kawate H, Nawata H, Takayanagi R. Glucocorticoid suppresses the canonical Wnt signal in cultured human osteoblasts. *Biochem Biophys Res Commun*. 2005;329(1):177-181. doi:10.1016/j.bbrc.2005.01.117

16. Swanson C, Lorentzon M, Conaway HH, Lerner UH. Glucocorticoid regulation of osteoclast differentiation and expression of receptor activator of nuclear factor-kappaB (NF-kappaB) ligand, osteoprotegerin, and receptor activator of NF-kappaB in mouse calvarial bones. *Endocrinology*. 2006;147(7):3613-3622. doi:10.1210/en.2005-0717

17. Mazziotti G, Formenti AM, Adler RA, et al. Glucocorticoid-induced osteoporosis: pathophysiological role of GH/IGF-I and PTH/VITAMIN D axes, treatment options and guidelines. *Endocrine*. 2016;54(3):603-611. doi:10.1007/s12020-016-1146-8

18. Sözen T, Özışık L, Başaran NÇ. An overview and management of osteoporosis. *Eur J Rheumatol*. 2017;4(1):46-56. doi:10.5152/eurjrheum.2016.048

19. Gennari L, Bilezikian JP. Osteoporosis in men. *Endocrinol Metab Clin North Am*. 2007;36(2):399-419. doi:10.1016/j.ecl.2007.03.008

20. Kanis JA, Oden A, Johnell O, De Laet C, Jonsson B, Oglesby AK. The components of excess mortality after hip fracture. *Bone*. 2003;32(5):468-473. doi:10.1016/s8756-3282(03)00061-9

21. Rao SS, Budhwar N, Ashfaque A. Osteoporosis in Men. *Am Fam Physician*. 2010;82(5):503-508.

22. Cosman F. Anabolic and antiresorptive therapy for osteoporosis: combination and sequential approaches. *Curr Osteoporos Rep*. 2014;12(4):385-395. doi:10.1007/s11914-014-0237-9

23. Lewiecki EM. Bisphosphonates for the treatment of osteoporosis: insights for clinicians. *Ther Adv Chronic Dis*. 2010;1(3):115-128. doi:10.1177/2040622310374783

24. O'Halloran M, Boyd NM, Smith A. Denosumab and osteonecrosis of the jaws - the pharmacology, pathogenesis and a report of two cases. *Aust Dent J*. 2014;59(4):516-519. doi:10.1111/adj.12217

25. Srinivasan A, Wong FK, Karponis D. Calcitonin: A useful old friend. *J Musculoskelet Neuronal Interact*. 2020;20(4):600-609.

26. Gambacciani M, Levancini M. Hormone replacement therapy and the prevention of postmenopausal osteoporosis. *Przegląd Menopauzalny Menopause Rev*. 2014;13(4):213-220. doi:10.5114/pm.2014.44996

27. Gennari L, Merlotti D, Nuti R. Selective estrogen receptor modulator (SERM) for the treatment of osteoporosis in postmenopausal women: focus on lasofoxifene. *Clin Interv Aging*. 2010;5:19-29.

28. Lindsay R, Krege JH, Marin F, Jin L, Stepan JJ. Teriparatide for osteoporosis: importance of the full course. *Osteoporos Int*. 2016;27(8):2395-2410. doi:10.1007/s00198-016-3534-6

29. McClung MR, Bolognese MA, Brown JP, et al. Skeletal responses to romosozumab after 12 months of denosumab. *JBMR Plus*. 2021;5(7):e10512. doi:10.1002/jbm4.10512

30. Marie PJ. Strontium ranelate: a dual mode of action rebalancing bone turnover in favour of bone formation. *Curr Opin Rheumatol*. 2006;18 Suppl 1:S11-15. doi:10.1097/01.bor.0000229522.89546.7b

31. Hamdy NAT. Strontium ranelate improves bone microarchitecture in osteoporosis. *Rheumatology*. 2009;48(suppl 4):iv9-iv13. doi:10.1093/rheumatology/kep274

32. Osborne V, Layton D, Perrio M, Wilton L, Shakir SAW. Incidence of Venous Thromboembolism in Users of Strontium Ranelate. *Drug Saf*. 2010;33(7):579-591. doi:10.2165/11533770-000000000-00000

33. Manolagas SC. Wnt signaling and osteoporosis. *Maturitas*. 2014;78(3):233-237. doi:10.1016/j.maturitas.2014.04.013

34. Clevers H. Wnt/β-Catenin Signaling in Development and Disease. *Cell*. 2006;127(3):469-480. doi:10.1016/j.cell.2006.10.018

35. Kikuchi A, Yamamoto H, Sato A. Selective activation mechanisms of Wnt signaling pathways. *Trends Cell Biol*. 2009;19(3):119-129. doi:10.1016/j.tcb.2009.01.003

36. Lerner UH, Ohlsson C. The WNT system: background and its role in bone. *J Intern Med*. 2015;277(6):630-649. doi:10.1111/joim.12368

37. Baron R, Gori F. Targeting WNT signaling in the treatment of osteoporosis. *Curr Opin Pharmacol*. 2018;40:134-141. doi:10.1016/j.coph.2018.04.011

38. Rodda SJ, McMahon AP. Distinct roles for Hedgehog and canonical Wnt signaling in specification, differentiation and maintenance of osteoblast progenitors. *Dev Camb Engl*. 2006;133(16):3231-3244. doi:10.1242/dev.02480

39. Almeida M, Han L, Bellido T, Manolagas SC, Kousteni S. Wnt proteins prevent apoptosis of both uncommitted osteoblast progenitors and differentiated osteoblasts by beta-catenin-dependent and -independent signaling cascades

involving Src/ERK and phosphatidylinositol 3-kinase/AKT. *J Biol Chem*. 2005;280(50):41342-41351. doi:10.1074/jbc.M502168200

40. Glass DA, Bialek P, Ahn JD, et al. Canonical Wnt signaling in differentiated osteoblasts controls osteoclast differentiation. *Dev Cell*. 2005;8(5):751-764. doi:10.1016/j.devcel.2005.02.017

41. Wei W, Zeve D, Suh JM, et al. Biphasic and Dosage-Dependent Regulation of Osteoclastogenesis by β-Catenin ▿. *Mol Cell Biol*. 2011;31(23):4706-4719. doi:10.1128/MCB.05980-11

42. Bennett CN, Ouyang H, Ma YL, et al. Wnt10b increases postnatal bone formation by enhancing osteoblast differentiation. *J Bone Miner Res Off J Am Soc Bone Miner Res*. 2007;22(12):1924-1932. doi:10.1359/jbmr.070810

43. Cawthorn WP, Bree AJ, Yao Y, et al. Wnt6, Wnt10a and Wnt10b inhibit adipogenesis and stimulate osteoblastogenesis through a β-catenin-dependent mechanism. *Bone*. 2012;50(2):477-489. doi:10.1016/j.bone.2011.08.010

44. Laine CM, Joeng KS, Campeau PM, et al. WNT1 Mutations in Early-onset Osteoporosis and Osteogenesis Imperfecta. *N Engl J Med*. 2013;368(19):1809-1816. doi:10.1056/NEJMoa1215458

45. Movérare-Skrtic S, Henning P, Liu X, et al. Osteoblast-derived WNT16 represses osteoclastogenesis and prevents cortical bone fragility fractures. *Nat Med*. 2014;20(11):1279-1288. doi:10.1038/nm.3654

46. Williams BO, Insogna KL. Where Wnts Went: The Exploding Field of Lrp5 and Lrp6 Signaling in Bone. *J Bone Miner Res*. 2009;24(2):171-178. doi:10.1359/jbmr.081235

47. Li X, Ominsky MS, Niu QT, et al. Targeted deletion of the sclerostin gene in mice results in increased bone formation and bone strength. *J Bone Miner Res Off J Am Soc Bone Miner Res*. 2008;23(6):860-869. doi:10.1359/jbmr.080216

48. Gaur T, Lengner CJ, Hovhannisyan H, et al. Canonical WNT signaling promotes osteogenesis by directly stimulating Runx2 gene expression. *J Biol Chem*. 2005;280(39):33132-33140. doi:10.1074/jbc.M500608200

49. Sato MM, Nakashima A, Nashimoto M, Yawaka Y, Tamura M. Bone morphogenetic protein-2 enhances Wnt/β-catenin signaling-induced osteoprotegerin expression. *Genes Cells*. 2009;14(2):141-153. doi:10.1111/j.1365-2443.2008.01258.x

50. Wnt co-receptors Lrp5 and Lrp6 differentially mediate Wnt3a signaling in osteoblasts | PLOS ONE. Accessed October 1, 2022. https://journals.plos.org/plosone/article?id=10.1371/journal.pone.0188264

51. Yu B, Chang J, Liu Y, et al. Wnt4 signaling prevents skeletal aging and inflammation by inhibiting nuclear factor-κB. *Nat Med*. 2014;20(9):1009-1017. doi:10.1038/nm.3586

52. Gu Q, Tian H, Zhang K, et al. Wnt5a/FZD4 Mediates the Mechanical Stretch-Induced Osteogenic Differentiation of Bone Mesenchymal Stem Cells. *Cell Physiol Biochem*. 2018;48(1):215-226. doi:10.1159/000491721

53. Tu X, Joeng KS, Nakayama KI, et al. Noncanonical Wnt Signaling through G Protein-Linked PKCδ Activation Promotes Bone Formation. *Dev Cell*. 2007;12(1):113-127. doi:10.1016/j.devcel.2006.11.00

54. Cruciat CM, Niehrs C. Secreted and Transmembrane Wnt Inhibitors and Activators. *Cold Spring Harb Perspect Biol*. 2013;5(3):a015081. doi:10.1101/cshperspect.a015081

55. Schepeler T. Emerging roles of microRNAs in the Wnt signaling network. *Crit Rev Oncog*. 2013;18(4):357-371. doi:10.1615/critrevoncog.2013006128

56. Lu TX, Rothenberg ME. MicroRNA. *J Allergy Clin Immunol*. 2018;141(4):1202-1207. doi:10.1016/j.jaci.2017.08.034

57. He L, Hannon GJ. MicroRNAs: small RNAs with a big role in gene regulation. *Nat Rev Genet*. 2004;5(7):522-531. doi:10.1038/nrg1379

58. Ha TY. MicroRNAs in Human Diseases: From Autoimmune Diseases to Skin, Psychiatric and Neurodegenerative Diseases. *Immune Netw*. 2011;11(5):227-244. doi:10.4110/in.2011.11.5.227

59. Bartel DP. MicroRNA Target Recognition and Regulatory Functions. *Cell*. 2009;136(2):215-233. doi:10.1016/j.cell.2009.01.002

60. Saxena S, Jónsson ZO, Dutta A. Small RNAs with imperfect match to endogenous mRNA repress translation. Implications for off-target activity of small inhibitory RNA in mammalian cells. *J Biol Chem*. 2003;278(45):44312-44319. doi:10.1074/jbc.M307089200

61. Baumann V, Winkler J. miRNA-based therapies: Strategies and delivery platforms for oligonucleotide and non-oligonucleotide agents. *Future Med Chem*. 2014;6(17):1967-1984. doi:10.4155/fmc.14.116

62. Lee Y, Kim M, Han J, et al. MicroRNA genes are transcribed by RNA polymerase II. *EMBO J*. 2004;23(20):4051-4060. doi:10.1038/sj.emboj.7600385

63. Han J, Lee Y, Yeom KH, et al. Molecular basis for the recognition of primary microRNAs by the Drosha-DGCR8 complex. *Cell*. 2006;125(5):887-901. doi:10.1016/j.cell.2006.03.043

64. Lee Y, Jeon K, Lee JT, Kim S, Kim VN. MicroRNA maturation: stepwise processing and subcellular localization. *EMBO J*. 2002;21(17):4663-4670. doi:10.1093/emboj/cdf476

65. Ketting RF, Fischer SEJ, Bernstein E, Sijen T, Hannon GJ, Plasterk RHA. Dicer functions in RNA interference and in synthesis of small RNA involved in developmental timing in C. elegans. *Genes Dev*. 2001;15(20):2654-2659. doi:10.1101/gad.927801

66. Hutvagner G. Small RNA asymmetry in RNAi: function in RISC assembly and gene regulation. *FEBS Lett*. 2005;579(26):5850-5857. doi:10.1016/j.febslet.2005.08.071

67. Valencia-Sanchez MA, Liu J, Hannon GJ, Parker R. Control of translation and mRNA degradation by miRNAs and siRNAs. *Genes Dev*. 2006;20(5):515-524. doi:10.1101/gad.1399806

68. Weber JA, Baxter DH, Zhang S, et al. The MicroRNA Spectrum in 12 Body Fluids. *Clin Chem*. 2010;56(11):1733-1741. doi:10.1373/clinchem.2010.147405

69. Henry JC, Azevedo-Pouly ACP, Schmittgen TD. MicroRNA replacement therapy for cancer. *Pharm Res*. 2011;28(12):3030-3042. doi:10.1007/s11095-011-0548-9

70. Lennox KA, Behlke MA. Chemical modification and design of anti-miRNA oligonucleotides. *Gene Ther*. 2011;18(12):1111-1120. doi:10.1038/gt.2011.100

71. Kasinski AL, Slack FJ. Arresting the Culprit: Targeted Antagomir Delivery to Sequester Oncogenic miR-221 in HCC. *Mol Ther Nucleic Acids*. 2012;1(3):e12. doi:10.1038/mtna.2012.2

72. Lin M, Hu X, Chang S, et al. Advances of Antisense Oligonucleotide Technology in the Treatment of Hereditary Neurodegenerative Diseases. *Evid-Based Complement Altern Med ECAM*. 2021;2021:6678422. doi:10.1155/2021/6678422

73. Lima JF, Cerqueira L, Figueiredo C, Oliveira C, Azevedo NF. Anti-miRNA oligonucleotides: A comprehensive guide for design. *RNA Biol*. 2018;15(3):338-352. doi:10.1080/15476286.2018.1445959

74. Pizzino G, Irrera N, Galfo F, et al. Effects of the antagomiRs 15b and 200b on the altered healing pattern of diabetic mice. *Br J Pharmacol*. 2018;175(4):644-655. doi:10.1111/bph.14113

75. Song JL, Nigam P, Tektas SS, Selva E. microRNA regulation of Wnt signaling pathways in development and disease. *Cell Signal*. 2015;27(7):1380-1391. doi:10.1016/j.cellsig.2015.03.018

76. Sun Q, Liu S, Feng J, Kang Y, Zhou Y, Guo S. Current Status of MicroRNAs that Target the Wnt Signaling Pathway in Regulation of Osteogenesis and Bone Metabolism: A Review. *Med Sci Monit Int Med J Exp Clin Res*. 2021;27:e929510-1-e929510-8. doi:10.12659/MSM.929510

77. He C, Liu M, Ding Q, Yang F, Xu T. Upregulated miR-9-5p inhibits osteogenic differentiation of bone marrow mesenchymal stem cells under high glucose treatment. *J Bone Miner Metab*. 2022;40(2):208-219. doi:10.1007/s00774-021-01280-9

78. Zhang HG, Wang XB, Zhao H, Zhou CN. MicroRNA-9-5p promotes osteoporosis development through inhibiting osteogenesis and promoting adipogenesis via targeting Wnt3a. *Eur Rev Med Pharmacol Sci*. 2019;23(2):456-463. doi:10.26355/eurrev_201901_16855

79. Jin Y, Peng D, Shen Y, et al. MicroRNA-376c inhibits cell proliferation and invasion in osteosarcoma by targeting to transforming growth factor-alpha. *DNA Cell Biol*. 2013;32(6):302-309. doi:10.1089/dna.2013.1977

80. Kureel J, John AA, Prakash R, Singh D. MiR 376c inhibits osteoblastogenesis by targeting Wnt3 and ARF-GEF-1 -facilitated augmentation of beta-catenin transactivation. *J Cell Biochem*. 2018;119(4):3293-3303. doi:10.1002/jcb.26490

81. Xu Y, Zhang S, Fu D, Lu D. Circulating miR-374b-5p negatively regulates osteoblast differentiation in the progression of osteoporosis via targeting Wnt3 AND Runx2. *J Biol Regul Homeost Agents*. 2020;34(2):345-355. doi:10.23812/19-507-A-9

82. Hashimi ST, Fulcher JA, Chang MH, Gov L, Wang S, Lee B. MicroRNA profiling identifies miR-34a and miR-21 and their target genes JAG1 and WNT1 in the coordinate regulation of dendritic cell differentiation. *Blood*. 2009;114(2):404-414. doi:10.1182/blood-2008-09-179150

83. Chen L, Holmstrøm K, Qiu W, et al. MicroRNA-34a inhibits osteoblast differentiation and in vivo bone formation of human stromal stem cells. *Stem Cells Dayt Ohio*. 2014;32(4):902-912. doi:10.1002/stem.1615

84. Deng Y, Wu S, Zhou H, et al. Effects of a miR-31, Runx2, and Satb2 regulatory loop on the osteogenic differentiation of bone mesenchymal stem cells. *Stem Cells Dev*. 2013;22(16):2278-2286. doi:10.1089/scd.2012.0686

85. Mizoguchi F, Murakami Y, Saito T, Miyasaka N, Kohsaka H. miR-31 controls osteoclast formation and bone resorption by targeting RhoA. *Arthritis Res Ther*. 2013;15(5):R102. doi:10.1186/ar4282

86. Weilner S, Schraml E, Wieser M, et al. Secreted microvesicular miR-31 inhibits osteogenic differentiation of mesenchymal stem cells. *Aging Cell*. 2016;15(4):744-754. doi:10.1111/acel.12484

87. Mäkitie RE, Hackl M, Niinimäki R, Kakko S, Grillari J, Mäkitie O. Altered MicroRNA Profile in Osteoporosis Caused by Impaired WNT Signaling. *J Clin Endocrinol Metab*. 2018;103(5):1985-1996. doi:10.1210/jc.2017-02585

88. Weigl M, Kocijan R, Ferguson J, et al. Longitudinal Changes of Circulating miRNAs During Bisphosphonate and Teriparatide Treatment in an Animal Model of Postmenopausal Osteoporosis. *J Bone Miner Res*. 2021;36(6):1131-1144. doi:10.1002/jbmr.4276

89. Heilmeier U, Hackl M, Schroeder F, et al. Circulating serum microRNAs including senescent miR-31-5p are associated with incident fragility fractures in older postmenopausal women with type 2 diabetes mellitus. *Bone*. 2022;158:116308. doi:10.1016/j.bone.2021.116308

90. Alexander MS, Kawahara G, Motohashi N, et al. MicroRNA-199a is induced in dystrophic muscle and affects WNT signaling, cell proliferation, and myogenic differentiation. *Cell Death Differ*. 2013;20(9):1194-1208. doi:10.1038/cdd.2013.62

91. Guo K, Zhang D, Wu H, Zhu Q, Yang C, Zhu J. MiRNA-199a-5p positively regulated RANKL-induced osteoclast differentiation by target Mafb protein. *J Cell Biochem*. Published online November 1, 2018. doi:10.1002/jcb.27968

92. Qi XB, Jia B, Wang W, et al. Role of miR-199a-5p in osteoblast differentiation by targeting TET2. *Gene*. 2020;726:144193. doi:10.1016/j.gene.2019.144193

93. Ding W, Ding S, Li J, et al. Aberrant Expression of miR-100 in Plasma of Patients with Osteoporosis and its Potential Diagnostic Value. *Clin Lab*. 2019;65(9). doi:10.7754/Clin.Lab.2019.190327

94. Dole NS, Yoon J, Monteiro DA, et al. Mechanosensitive miR-100 coordinates TGFβ and Wnt signaling in osteocytes during fluid shear stress. *FASEB J Off Publ Fed Am Soc Exp Biol*. 2021;35(10):e21883. doi:10.1096/fj.202100930

95. Duan L, Zhao H, Xiong Y, et al. miR-16-2* Interferes with WNT5A to Regulate Osteogenesis of Mesenchymal Stem Cells. *Cell Physiol Biochem Int J Exp Cell Physiol Biochem Pharmacol*. 2018;51(3):1087-1102. doi:10.1159/000495489

96. Du F, Wu H, Zhou Z, Liu YU. microRNA-375 inhibits osteogenic differentiation by targeting runt-related transcription factor 2. *Exp Ther Med*. 2015;10(1):207-212. doi:10.3892/etm.2015.2477

97. Wang Y, Huang C, Reddy Chintagari N, et al. miR-375 regulates rat alveolar epithelial cell trans-differentiation by inhibiting Wnt/β-catenin pathway. *Nucleic Acids Res*. 2013;41(6):3833-3844. doi:10.1093/nar/gks1460

98. Kim DK, Bandara G, Cho YE, et al. Mastocytosis-derived extracellular vesicles deliver miR-23a and miR-30a into pre-osteoblasts and prevent osteoblastogenesis and bone formation. *Nat Commun*. 2021;12:2527. doi:10.1038/s41467-021-22754-4

99. Li T, Li H, Wang Y, et al. microRNA-23a inhibits osteogenic differentiation of human bone marrow-derived mesenchymal stem cells by targeting LRP5. *Int J Biochem Cell Biol*. 2016;72:55-62. doi:10.1016/j.biocel.2016.01.004

100. Prakash R, John AA, Singh D. miR-409-5p negatively regulates Wnt/Beta catenin signaling pathway by targeting Lrp-8. *J Cell Physiol*. 2019;234(12):23507-23517. doi:10.1002/jcp.28919

101. Wang X, Guo B, Li Q, et al. miR-214 targets ATF4 to inhibit bone formation. *Nat Med*. 2013;19(1):93-100. doi:10.1038/nm.3026

102. Li JP, Zhuang HT, Xin MY, Zhou YL. MiR-214 inhibits human mesenchymal stem cells differentiating into osteoblasts through targeting β-catenin. *Eur Rev Med Pharmacol Sci*. 2017;21(21):4777-4783.

103. Yi SJ, Li LL, Tu WB. MiR-214 negatively regulates proliferation and WNT/β-catenin signaling in breast cancer. *Eur Rev Med Pharmacol Sci*. 2016;20(24):5148-5154.

104. Long H, Sun B, Cheng L, et al. miR-139-5p Represses BMSC Osteogenesis via Targeting Wnt/β-Catenin Signaling Pathway. *DNA Cell Biol*. 2017;36(8):715-724. doi:10.1089/dna.2017.3657

105. Feng Y, Wan P, Yin L, Lou X. The Inhibition of MicroRNA-139-5p Promoted Osteoporosis of Bone Marrow-Derived Mesenchymal Stem Cells by Targeting Wnt/Beta-Catenin Signaling Pathway by NOTCH1. *J Microbiol Biotechnol*. 2020;30(3):448-458. doi:10.4014/jmb.1908.08036

106. Liang WC, Fu WM, Wang YB, et al. H19 activates Wnt signaling and promotes osteoblast differentiation by functioning as a competing endogenous RNA. *Sci Rep*. 2016;6:20121. doi:10.1038/srep20121

107. Qiu W, Kassem M. miR-141-3p inhibits human stromal (mesenchymal) stem cell proliferation and differentiation. *Biochim Biophys Acta BBA - Mol Cell Res*. 2014;1843(9):2114-2121. doi:10.1016/j.bbamcr.2014.06.004

108. Lin Y, Xiao L, Zhang Y, Li P, Wu Y, Lin Y. MiR-26b-3p regulates osteoblast differentiation via targeting estrogen receptor α. *Genomics*. 2019;111(5):1089-1096. doi:10.1016/j.ygeno.2018.07.003

109. Hu H, Zhao C, Zhang P, et al. miR-26b modulates OA induced BMSC osteogenesis through regulating GSK3β/β-catenin pathway. *Exp Mol Pathol*. 2019;107:158-164. doi:10.1016/j.yexmp.2019.02.003

110. Wang Q, Cai J, Cai X hua, Chen L. miR-346 Regulates Osteogenic Differentiation of Human Bone Marrow-Derived Mesenchymal Stem Cells by Targeting the Wnt/β-Catenin Pathway. *PLoS ONE*. 2013;8(9):e72266. doi:10.1371/journal.pone.0072266

111. Hu W, Ye Y, Zhang W, Wang J, Chen A, Guo F. miR-142-3p promotes osteoblast differentiation by modulating Wnt signaling. *Mol Med Rep*. 2013;7(2):689-693. doi:10.3892/mmr.2012.1207

112. Guo D, Li Q, Lv Q, Wei Q, Cao S, Gu J. MiR-27a Targets sFRP1 in hFOB Cells to Regulate Proliferation, Apoptosis and Differentiation. *PLoS ONE*. 2014;9(3):e91354. doi:10.1371/journal.pone.0091354

113. Wang T, Xu Z. miR-27 promotes osteoblast differentiation by modulating Wnt signaling. *Biochem Biophys Res Commun*. 2010;402(2):186-189. doi:10.1016/j.bbrc.2010.08.031

114. Hassan MQ, Maeda Y, Taipaleenmaki H, et al. miR-218 Directs a Wnt Signaling Circuit to Promote Differentiation of Osteoblasts and Osteomimicry of Metastatic Cancer Cells. *J Biol Chem*. 2012;287(50):42084-42092. doi:10.1074/jbc.M112.377515

115. Karimi Z, Seyedjafari E, Khojasteh A, Hashemi SM, Kazemi B, Mohammadi-Yeganeh S. MicroRNA-218 competes with differentiation media in the induction of osteogenic differentiation of mesenchymal stem cell by regulating β-catenin inhibitors. *Mol Biol Rep*. 2020;47(11):8451-8463. doi:10.1007/s11033-020-05885-7

116. Zhang WB, Zhong WJ, Wang L. A signal-amplification circuit between miR-218 and Wnt/β-catenin signal promotes human adipose tissue-derived stem cells osteogenic differentiation. *Bone*. 2014;58:59-66. doi:10.1016/j.bone.2013.09.015

117. Ko JY, Chuang PC, Ke HJ, Chen YS, Sun YC, Wang FS. MicroRNA-29a mitigates glucocorticoid induction of bone loss and fatty marrow by rescuing Runx2 acetylation. *Bone*. 2015;81:80-88. doi:10.1016/j.bone.2015.06.022

118. Kapinas K, Kessler C, Ricks T, Gronowicz G, Delany AM. miR-29 Modulates Wnt Signaling in Human Osteoblasts through a Positive Feedback Loop. *J Biol Chem*. 2010;285(33):25221-25231. doi:10.1074/jbc.M110.116137

119. Li ZH, Hu H, Zhang XY, et al. MiR-291a-3p regulates the BMSCs differentiation via targeting DKK1 in dexamethasone-induced osteoporosis. *Kaohsiung J Med Sci*. 2020;36(1):35-42. doi:10.1002/kjm2.12134

120. Tang X, Lin J, Wang G, Lu J. MicroRNA-433-3p promotes osteoblast differentiation through targeting DKK1 expression. *PLoS ONE*. 2017;12(6):e0179860. doi:10.1371/journal.pone.0179860

121. Zhang L, Tang Y, Zhu X, et al. Overexpression of MiR-335-5p Promotes Bone Formation and Regeneration in Mice. *J Bone Miner Res Off J Am Soc Bone Miner Res*. 2017;32(12):2466-2475. doi:10.1002/jbmr.3230

122. Li J, Feng Z, Chen L, Wang X, Deng H. MicroRNA-335-5p inhibits osteoblast apoptosis induced by high glucose. *Mol Med Rep*. 2016;13(5):4108-4112. doi:10.3892/mmr.2016.4994

123. Li S, Yin Y, Yao L, et al. TNF-α treatment increases DKK1 protein levels in primary osteoblasts via upregulation of DKK1 mRNA levels and downregulation of miR-335-5p. *Mol Med Rep*. 2020;22(2):1017-1025. doi:10.3892/mmr.2020.11152

124. Zhu XB, Lin WJ, Lv C, et al. MicroRNA-539 promotes osteoblast proliferation and differentiation and osteoclast apoptosis through the AXNA-dependent Wnt signaling pathway in osteoporotic rats. *J Cell Biochem*. 2018;119(10):8346-8358. doi:10.1002/jcb.26910

125. Zhang X, Zhu Y, Zhang C, et al. miR-542-3p prevents ovariectomy-induced osteoporosis in rats via targeting SFRP1. *J Cell Physiol*. 2018;233(9):6798-6806. doi:10.1002/jcp.26430

126. Ma Y, Shen N, Wicha MS, Luo M. The Roles of the Let-7 Family of MicroRNAs in the Regulation of Cancer Stemness. *Cells*. 2021;10(9):2415. doi:10.3390/cells10092415

127. Wei J, Li H, Wang S, et al. let-7 Enhances Osteogenesis and Bone Formation While Repressing Adipogenesis of Human Stromal/Mesenchymal Stem Cells by Regulating HMGA2. *Stem Cells Dev*. 2014;23(13):1452-1463. doi:10.1089/scd.2013.0600

128. Wang Y, Zhao J, Chen S, et al. Let-7 as a Promising Target in Aging and Aging-Related Diseases: A Promise or a Pledge. *Biomolecules*. 2022;12(8):1070. doi:10.3390/biom12081070

129. Zhou Z, Lu Y, Wang Y, Du L, Zhang Y, Tao J. Let-7c regulates proliferation and osteodifferentiation of human adipose-derived mesenchymal stem cells under oxidative stress by targeting SCD-1. *Am J Physiol-Cell Physiol*. 2019;316(1):C57-C69. doi:10.1152/ajpcell.00211.2018

130. Luo Y, Ge R, Wu H, et al. The osteogenic differentiation of human adipose-derived stem cells is regulated through the let-7i-3p/LEF1/β-catenin axis under cyclic strain. *Stem Cell Res Ther*. 2019;10(1):339. doi:10.1186/s13287-019-1470-z

131. Chen YN, Ren CC, Yang L, et al. MicroRNA let-7d-5p rescues ovarian cancer cell apoptosis and restores chemosensitivity by regulating the p53 signaling pathway via HMGA1. *Int J Oncol*. 2019;54(5):1771-1784. doi:10.3892/ijo.2019.4731

132. Jia WQ, Zhu JW, Yang CY, et al. Verbascoside inhibits progression of glioblastoma cells by promoting Let-7g-5p and down-regulating HMGA2 via Wnt/beta-catenin signalling blockade. *J Cell Mol Med*. 2020;24(5):2901-2916. doi:10.1111/jcmm.14884

133. Komori T. Animal models for osteoporosis. *Eur J Pharmacol*. 2015;759:287-294. doi:10.1016/j.ejphar.2015.03.028

134. Lelovas PP, Xanthos TT, Thoma SE, Lyritis GP, Dontas IA. The Laboratory Rat as an Animal Model for Osteoporosis Research. *Comp Med*. 2008;58(5):424-430.

135. Wood CL, Soucek O, Wong SC, et al. Animal models to explore the effects of glucocorticoids on skeletal growth and structure. *J Endocrinol*. 2018;236(1):R69-R91. doi:10.1530/JOE-17-0361

136. Yao W, Cheng Z, Pham A, et al. Glucocorticoid-induced bone loss in mice can be reversed by the actions of parathyroid hormone and risedronate on different pathways for bone formation and mineralization. *Arthritis Rheum*. 2008;58(11):3485-3497. doi:10.1002/art.23954

137. Campbell JM, Bacon TA, Wickstrom E. Oligodeoxynucleoside phosphorothioate stability in subcellular extracts, culture media, sera and cerebrospinal fluid. *J Biochem Biophys Methods*. 1990;20(3):259-267. doi:10.1016/0165-022x(90)90084-p

138. Geary RS, Norris D, Yu R, Bennett CF. Pharmacokinetics, biodistribution and cell uptake of antisense oligonucleotides. *Adv Drug Deliv Rev*. 2015;87:46-51. doi:10.1016/j.addr.2015.01.008

139. Miller CM, Donner AJ, Blank EE, et al. Stabilin-1 and Stabilin-2 are specific receptors for the cellular internalization of phosphorothioate-modified antisense oligonucleotides (ASOs) in the liver. *Nucleic Acids Res*. 2016;44(6):2782-2794. doi:10.1093/nar/gkw112

140. Straarup EM, Fisker N, Hedtjärn M, et al. Short locked nucleic acid antisense oligonucleotides potently reduce apolipoprotein B mRNA and serum cholesterol in mice and non-human primates. *Nucleic Acids Res*. 2010;38(20):7100-7111. doi:10.1093/nar/gkq457

141. Hernlund E, Svedbom A, Ivergård M, et al. Osteoporosis in the European Union: medical management, epidemiology and economic burden. *Arch Osteoporos*. 2013;8(1):136. doi:10.1007/s11657-013-0136-1

142. Panday K, Gona A, Humphrey MB. Medication-induced osteoporosis: screening and treatment strategies. *Ther Adv Musculoskelet Dis*. 2014;6(5):185-202. doi:10.1177/1759720X14546350

143. Harvey N, Dennison E, Cooper C. Osteoporosis: impact on health and economics. *Nat Rev Rheumatol*. 2010;6(2):99-105. doi:10.1038/nrrheum.2009.260

144. Papaioannou A, Kennedy CC, Dolovich L, Lau E, Adachi JD. Patient adherence to osteoporosis medications: problems, consequences and management strategies. *Drugs Aging*. 2007;24(1):37-55. doi:10.2165/00002512-200724010-00003

145. Canalis E. Wnt signalling in osteoporosis: mechanisms and novel therapeutic approaches. *Nat Rev Endocrinol*. 2013;9(10):575-583. doi:10.1038/nrendo.2013.154

146. Yang Y, Yujiao W, Fang W, et al. The roles of miRNA, lncRNA and circRNA in the development of osteoporosis. *Biol Res*. 2020;53:40. doi:10.1186/s40659-020-00309-z

147. Kaur T, Kapila R, Kapila S, Kaur T, Kapila R, Kapila S. *MicroRNAs as Next Generation Therapeutics in Osteoporosis*. IntechOpen; 2020. doi:10.5772/intechopen.91223

148. Friedman MS, Oyserman SM, Hankenson KD. Wnt11 Promotes Osteoblast Maturation and Mineralization through R-spondin 2*. *J Biol Chem*. 2009;284(21):14117-14125. doi:10.1074/jbc.M808337200

149. Zhu JH, Liao YP, Li FS, et al. Wnt11 promotes BMP9-induced osteogenic differentiation through BMPs/Smads and p38 MAPK in mesenchymal stem cells. *J Cell Biochem*. 2018;119(11):9462-9473. doi:10.1002/jcb.27262

150. Van Dijk FS, Nesbitt IM, Nikkels PGJ, et al. CRTAP mutations in lethal and severe osteogenesis imperfecta: the importance of combining biochemical and molecular genetic analysis. *Eur J Hum Genet*. 2009;17(12):1560-1569. doi:10.1038/ejhg.2009.75

151. Lojk J, Marc J. Roles of Non-Canonical Wnt Signalling Pathways in Bone Biology. *Int J Mol Sci*. 2021;22(19):10840. doi:10.3390/ijms221910840

152. Chen JF, Lin PW, Tsai YR, Yang YC, Kang HY. Androgens and Androgen Receptor Actions on Bone Health and Disease: From Androgen Deficiency to Androgen Therapy. *Cells*. 2019;8(11):1318. doi:10.3390/cells8111318

153. Wu J. Interactions of PTH and Wnt signaling in bone formation. Accessed October 9, 2022. https://grantome.com/grant/NIH/R01-AR073773-02

154. Schaller S, Henriksen K, Sveigaard C, et al. The Chloride Channel Inhibitor NS3736 Prevents Bone Resorption in Ovariectomized Rats Without Changing Bone Formation. *J Bone Miner Res*. 2004;19(7):1144-1153. doi:10.1359/JBMR.040302

155. Jiang L, Sheng K, Wang C, Xue D, Pan Z. The Effect of MMP-2 Inhibitor 1 on Osteogenesis and Angiogenesis During Bone Regeneration. *Front Cell Dev Biol*. 2021;8:596783. doi:10.3389/fcell.2020.596783

156. Xi G, Wai C, DeMambro V, Rosen CJ, Clemmons DR. IGFBP-2 directly stimulates osteoblast differentiation. *J Bone Miner Res Off J Am Soc Bone Miner Res*. 2014;29(11):2427-2438. doi:10.1002/jbmr.2282

157. Buccoliero C, Dicarlo M, Pignataro P, et al. The Novel Role of PGC1α in Bone Metabolism. *Int J Mol Sci*. 2021;22(9):4670. doi:10.3390/ijms22094670

158. Datta NS, Pettway GJ, Chen C, Koh AJ, McCauley LK. Cyclin D1 as a target for the proliferative effects of PTH and PTHrP in early osteoblastic cells. *J Bone Miner Res Off J Am Soc Bone Miner Res*. 2007;22(7):951-964. doi:10.1359/jbmr.070328

159. Gong H, Jarzynka MJ, Cole TJ, et al. Glucocorticoids Antagonize Estrogens by Glucocorticoid Receptor–Mediated Activation of Estrogen Sulfotransferase. *Cancer Res*. 2008;68(18):7386-7393. doi:10.1158/0008-5472.CAN-08-1545

160. Mohamed OA, Dufort D, Clarke HJ. Expression and Estradiol Regulation of Wnt Genes in the Mouse Blastocyst Identify a Candidate Pathway for Embryo-Maternal Signaling at Implantation1. *Biol Reprod*. 2004;71(2):417-424. doi:10.1095/biolreprod.103.025692

161. Dwyer MA, Joseph JD, Wade HE, et al. WNT11 expression is induced by estrogen-related receptor alpha and beta-catenin and acts in an autocrine manner to increase cancer cell migration. *Cancer Res*. 2010;70(22):9298-9308. doi:10.1158/0008-5472.CAN-10-0226

162. Hildebrandt S, Baschant U, Thiele S, Tuckermann J, Hofbauer LC, Rauner M. Glucocorticoids suppress Wnt16 expression in osteoblasts in vitro and in vivo. *Sci Rep*. 2018;8(1):8711. doi:10.1038/s41598-018-26300-z